GEOLOGICA BELGICA
2024, Vol. 27/1-2, 47–70
https://doi.org/10.20341/gb.2024.005

A Neogene succession in the city centre of Antwerp (Belgium): stratigraphy, palaeontology and geotechnics of the Rubenshuis temporary outcrop

STIJN EVERAERT

Royal Belgian Institute of Natural Sciences, OD Earth & History of Life, Vautierstraat 29, 1000 Brussels, Belgium; ***corresponding author:*** *stijn.everaert1@gmail.com.*

JEF DECKERS

VITO, Boeretang 200, 2400 Mol, Belgium; jef.deckers@vito.be.

MARK BOSSELAERS

Royal Belgian Institute of Natural Sciences, OD Earth & History of Life, Vautierstraat 29, 1000 Brussels, Belgium; Koninklijk Zeeuwsch Genootschap der Wetenschappen, PO Box 378, 4330 AJ Middelburg, the Netherlands; mark.bosselaers@telenet.be.

MARCO SCHILTZ

Samsuffit BVBA, Eggelstraat 8, 2530 Boechout, Belgium; marco@samsuffit.be.

STEPHEN LOUWYE

Paleontology and paleoenvironments, Department of Geology, Ghent University, Krijgslaan 281, 9000 Ghent, Belgium; stephen.louwye@ugent.be.

ABSTRACT

A temporary outcrop near the "Rubenshuis" in the centre of Antwerp (northern Belgium) facilitated the study of the Neogene glauconitic sand of the Berchem and Kattendijk formations, west and south of their respective stratotype sections. In contrast to the latter sections, the exposed Kiel Member of the Berchem Formation contains a relatively silty interval in its upper part, which is also reflected in Cone Penetration Tests. This silty interval is rich in molluscs, including the subspecies *Glossus lunulatus* cf. *lunulatus* and *Ennucula haesendoncki haesendoncki*, previously unknown from this member. Dinoflagellate cysts indicate that the main body of the Kiel Member was deposited during the middle Burdigalian, while only the upper part was deposited during the late Burdigalian. The Kiel Member is covered by the shell-rich, silty sand of the Langhian Antwerpen Member (Berchem Formation). Both members display soft-sediment deformation structures, probably caused by differences in silt content between and within these units. The Antwerpen Member is incised by the Lower Pliocene Kattendijk Formation, which reduced the thickness of the former to only 1.1 m, compared to 7 m in northeastern Antwerp. As a result, the basal gravel of the Kattendijk Formation contains many fossils reworked from the Antwerpen Member, in addition to autochthonous molluscs and *Ditrupa*. The Zanclean fauna resembles associations known from the highest part of the Kattendijk Formation in the former Oosterweel outcrop north of Antwerp, while it differs from the fauna of the lowermost Kattendijk Formation near Doel and Kallo. Hence, the palaeontological observations corroborate the regional depositional model of this unit, suggesting that only the youngest gully sequence of the Kattendijk Formation was deposited across the city of Antwerp.

KEYWORDS

Kiel Member,
Antwerpen Member,
Kattendijk Formation,
molluscs,
dinoflagellate cysts,
Miocene,
Pliocene,
Cone Penetration Tests

Article history

Received 19.03.2024, accepted in revised form 05.06.2024, available online 06.11.2024.

1. Introduction

Large parts of northern Belgium were covered by a shallow epicontinental sea during the Neogene, which resulted in the deposition of often fossiliferous, fine-grained sand with a varying amount of glauconite (Louwye et al., 2020a, 2020b). These Neogene deposits have been exposed near the city of Antwerp during infrastructure works and the excavation of harbour docks and sluices (e.g., Cogels, 1874; Van den Broeck, 1892; de Heinzelin de Braucourt, 1950, 1955; De Meuter et al., 1976; Goolaerts et al., 2020; Everaert et al., 2020), and displayed distinct lateral variations (Janssen & Van der Mark, 1968; Moorkens, 1969; De Meuter et al., 1976). Correlations using Cone Penetration Tests (CPTs) by Deckers & Louwye (2020) showed that the lower Pliocene Kattendijk Formation progressively truncated the lower to middle Miocene Berchem Formation in the western direction and eventually completely removed the latter just north of the city of Antwerp (Fig. 1). Within the Berchem Formation, Everaert et al. (2020) concluded that the upper Burdigalian part of the Kiel Member progressively thins and disappears from south to north in the city, based on extrapolations of biozone thickness trends across different temporary outcrops. However, while most outcrops in the Antwerp area have been studied near the Ring Road R1 (Fig. 1), considerably fewer sections were described in the city centre (De Meuter et al., 1976; Hoedemakers & Marquet, 2024). A temporary outcrop in the city centre can therefore further detail the findings of Deckers & Louwye (2020) and Everaert et al. (2020). In 2022, the construction pit of the new visitors' centre of the "Rubenshuis" in central Antwerp (Fig. 1) provided such an opportunity and allowed the investigation of the boundary between the Berchem Formation and the overlying Kattendijk Formation as well as their internal structure. This study documents the lithology, stratigraphy, palaeobiology and geotechnical properties of these units in the Rubenshuis outcrop, to complement the detailed understanding of the complex Neogene stratigraphic architecture and depositional history of the Antwerp area.

2. Geological background

The shallow marine Berchem Formation consists of dark-coloured, (very) glauconitic fine- to medium fine-grained sand with a varying content of clay and silt, shell beds and levels with phosphatic concretions (De Meuter & Laga, 1976; Louwye & Deckers, 2023). The sediments were deposited during an eustatic sea-level rise, when the sea started to progressively invade northern Belgium during the Aquitanian-early Burdigalian (Louwye, 2005; Munsterman & Deckers, 2020). In the Antwerp area, the Berchem Formation is divided into the Burdigalian Edegem and Kiel members and the Langhian–Serravallian Antwerpen Member (Louwye et al., 2000; 2020a). Although the lithology of the Kiel and Antwerpen members is rather similar with glauconite contents between 40–60%, the lower part of the Antwerpen Member is relatively enriched in silt and very fine-grained sand, probably linked to transgression during the Mid-Miocene Climatic Optimum (MMCO) (Deckers & Everaert, 2022; Deckers et al., 2023a). The erosional hiatus between both members spans parts of the late Burdigalian (Everaert et al., 2020). While the Kiel Member is often lacking shell beds and only locally contains some fragile shell concentrations and sandstones, the Antwerpen Member holds a succession of well-developed shell beds (De Meuter & Laga, 1976), some of which are continuous from at least Borgerhout to Borsbeek (Fig. 1) (Deckers & Everaert, 2022; Deckers & Goolaerts, 2022). After the Middle Miocene Unconformity (MMU), which spans the latest Serravallian and early Tortonian, the Berchem Formation became covered by the middle Tortonian Diest Formation, which is only locally preserved in northeastern Antwerp and the surroundings of Borsbeek (De Meuter et al., 1976; Goolaerts et al., 2020) (Fig. 1). The overlying Zanclean Kattendijk Formation is characterised by less glauconitic (15–25%, cf. Laga, 1972) fine- to medium fine-grained sand with shells and local concentrations of *Ditrupa* (De Meuter & Laga, 1976; Deckers et al., 2023b). Cogels (1874) introduced this unit as "*Sables à Isocardia cor*", a bivalve currently known as *Glossus humanus* (Linnaeus, 1758). The Kattendijk Formation is marked by an erosive basal gravel of rounded quartz and flints, together with shark's teeth, phosphatic nodules and rounded bone fragments (De Meuter & Laga, 1976). The Kattendijk Formation overlies in northeastern Antwerp a thick succession of the Antwerpen Member (De Meuter et al., 1976). Westward, the Kattendijk Formation gradually incises deeper into the Berchem Formation and ultimately completely removes the latter in the northwestern part of the city (Deckers & Louwye, 2020). As the Kattendijk

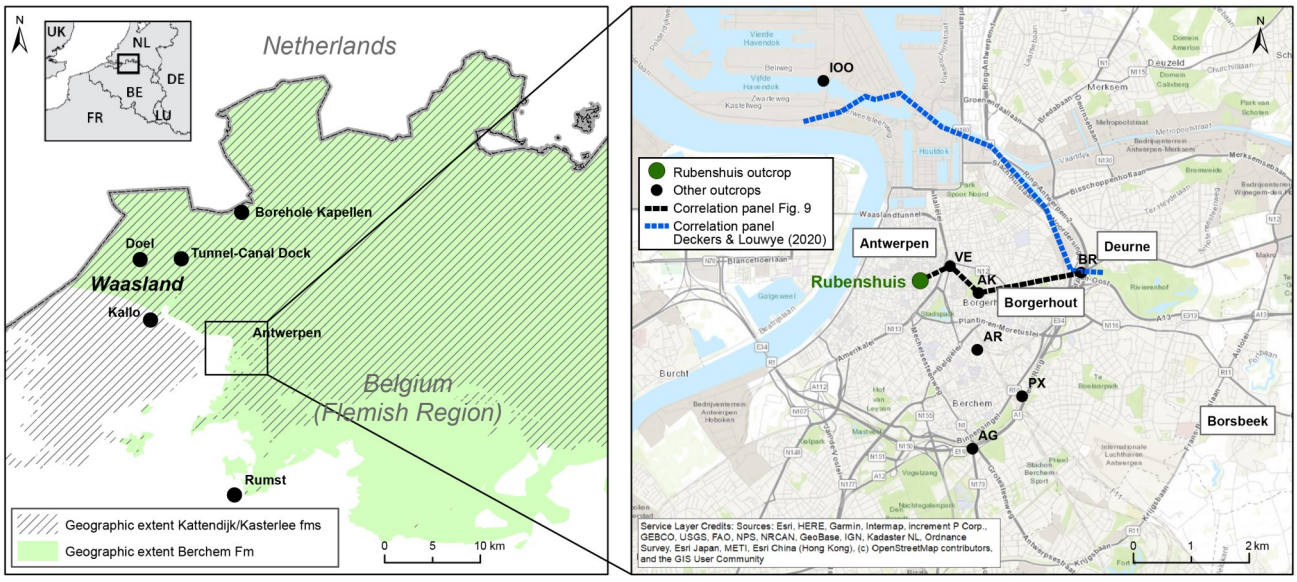

Figure 1. An overview of the study area with all locations mentioned in the text (see Table 1).

Formation incises deeper, it thickens and reaches a maximum of 15 m in a deep gully incision at the westernmost point of the correlation panel of Deckers & Louwye (2020) (Fig. 1). Deckers & Louwye (2020) identified two lithologically identical sequences within the Kattendijk Formation from Cone Penetration Tests. Both sequences have a transgressive basal gravel indicating erosive episodes. The composition of the basal gravels varies locally. Initially, the deepest gully in the Waasland area (Fig. 1) was filled with a lower sequence, followed by a second transgression filling a wider shallow gully system, the upper sequence (Deckers & Louwye, 2020).

3. Materials and methods

3.1. Locality and sampling

The Rubenshuis section (BGD 028W1009; DOV TO-20220706) is located in the city centre of Antwerp (WGS84 coordinates 51.2168, 4.4099, +7.3 m TAW Belgian Ordnance Datum) (Fig. 1). Sixteen (sub)samples are stored at the Geological Survey of Belgium (BGD) and the Geotheek of the Flemish Department of the Environment (VPO) (Supplementary data: Table S1). All sections discussed in this paper can be found in Table 1.

3.2. Cone Penetration Tests

Three electric Cone Penetration Tests (CPTs) were carried out in 2020 by Samsuffit Geo Service before the excavating works started. Cone resistance (qc) and local friction (fs) are measured by pushing an instrumented cone into the soil. These parameters and the derived friction ratio (Rf = fs/qc x 100) are traditionally used to determine soil type layering and are used in Figure 6 (CPT 2). Robertson (1990, 2010a, 2010b) further elaborated on these "classic" parameters and derived a normalised soil behaviour type (SBT) index Ic SBTn and a normalised hydraulic conductivity estimate k SBTn. Using normalised parameters is a better practice in general because both qc and fs tend to increase with depth due to the increase of overburden stress. Both Ic SBTn and k SBTn characterise the soil behaviour type as indicated in Figure 7. Schiltz (2020) demonstrated that these derived parameters show a close analogy with gamma-ray logs of Neogene sediments in the Campine area. Moreover, they often outperform the classical parameters qc and Rf in discerning and correlating stratigraphic units in sandy layers with low lithological contrast. For stratigraphic analysis, both the traditional CPT parameters qc and Rf (Figure 6) as well as the trends in the logs of the derived SBT parameters are used (Figure 7). The SBT parameters show fining and coarsening upward (FU and CU) trends or cycles, referred to as "SBT sequences". These should not be confused with "sequences" as defined and used in sequence stratigraphy.

3.3. Palynological preparation

Six samples (Fig. 2) were processed according to the procedure described in Louwye et al. (2004). The maceration involved a treatment with HCl for the removal of carbonates and a subsequent treatment with HF for the removal of silicates. A short ultrasonication for 15 s was carried out for an adequate dispersion. The residues were filtered on a nylon screen with a 16 µm mesh size and strew mounted on slides with glycerine jelly. The microscopic analysis was carried out with a Zeiss AxioImager A1 transmitted light microscope at 200x and 400x magnifications until a minimum of 250 palynomorphs were counted in non-overlapping traverses. The remainder of the slide was then counted for rare specimens. The nomenclature used is after Williams et al. (2017). The age-calibrated dinocyst zonation of Dybkjær & Piasecki (2010) for the eastern North Sea Basin is applied, which is compared to the zonation of de Verteuil & Norris (1996) erected in the eastern coastal plain of the USA.

3.4. Collection of macrofossils

Characteristic fossils were visually collected from the surface in each fossiliferous stratum. Sediment within the larger shells of the Kattendijk Formation was dried and sieved at mesh size 1 mm for the collection of smaller fossils. The Kiel Member was sampled by combining two methods: (1) larger amounts of sediment were sieved on site with a 5 mm mesh size, while (2) ca. 20 litres of layers B and E were sieved off-site with a 1 mm mesh to collect smaller specimens. Although the sampling was

Table 1. Overview of all localities (temporary outcrops and boreholes) mentioned in this study, their codes in Databank Ondergrond Vlaanderen (DOV), the Geological Survey of Belgium (BGD) and references to their lithological descriptions and lithostratigraphic interpretations.

Locality	Code DOV	Code BGD	Reference
Antwerpen – Rubenshuis (RU)	TO-20220706	028W1009	This study
Antwerpen – Argenta (AR)	TO-20190417	028W1004	Everaert et al. (2020)
Antwerpen – Van Ertbornstraat (VE)	/	/	Hoedemakers & Marquet (2024)
Antwerpen – Kievitstraat (AK)	kb15d28w-B453	028W0399	De Meuter et al. (1976)
Antwerpen – Oosterweel (IOO)	/	028W0876	Laga (1972); Ringelé (1974)
Antwerpen – Tunnel-Canal Dock	BGD015W0304	015W0304	Laga (1972); De Schepper et al. (2009)
Berchem – Grote Steenweg (AG)	kb15d28w-B451	028W0397	De Meuter et al. (1976)
Berchem – Post X (PX)	TO-20150701	028E0923	Everaert et al. (2019)
Borgerhout – Rivierenhof (BR)	kb15d28e-B580	028E0499	De Meuter et al. (1976)
Doel – Deurganckdock	TO-19991001	/	Louwye et al. (2004)
Kapellen – PIPDA borehole	DOV 1434-B-G227574-9_Kapellen3_WVP27	/	Deckers & Everaert (2023)
Rumst – Wienerberger quarry	TO-20211119	/	In preparation

relatively limited, the main components of the fauna are sufficiently represented.

All fossils are stored at the Royal Belgian Institute of Natural Sciences (RBINS) in Brussels (Belgium), palaeontology collection number IG 34663. The figured invertebrates are stored under collection numbers RBINS 7737–7753, two figured shark teeth have numbers RBINS P 10760–10761. For comparison, the Cenozoic mollusc collection of Naturalis Biodiversity Center (NBC) was consulted in Leiden (the Netherlands).

4. The Rubenshuis section

4.1. Lithology and lithostratigraphy

Eighteen lithological layers could be distinguished in the studied section (Fig. 2). See the Supplementary data for a detailed description and images of the samples (Fig. S1).

Layers A to N are characterised by predominantly fine-grained sand with a characteristic grey to dark grey and dark green colour (Figs 3–5), caused by a very high glauconite content (30–60%) (Fig. 6). Hence, they can be attributed to the Berchem Formation (De Meuter & Laga, 1976; Louwye & Deckers, 2023). The base of the Berchem Formation was not reached in the Rubenshuis outcrop.

Layers A-B-C are most characteristic of the Kiel Member: the intensely bioturbated (Fig. 4C), fine- to medium fine-grained sand has very little silty admixture, shows sporadic clay streaks (Fig. 4F) and only rarely contains some partially decalcified shells (Fig. 4D–E) (De Meuter & Laga, 1976; Louwye et al., 2023a). The overlying layers D-E-F are siltier and contain a well-developed shell bed (layer E, Fig. 4A–B, Fig. 5A). Due to its higher silt content (Fig. 6), this interval is atypical for the Kiel Member and even resembles the dominant facies of the younger Antwerpen Member (Louwye et al, 2023a; 2023b). However, the silt content decreases again in the overlying layer G (Fig. S1), which has a greyish colour, displays bioturbation (including some lithified *Ophiomorpha* in its top) and lacks calcareous macrofossils (Fig. 3D–E). Therefore, layer G can be interpreted as the top of the Kiel Member, in accordance with

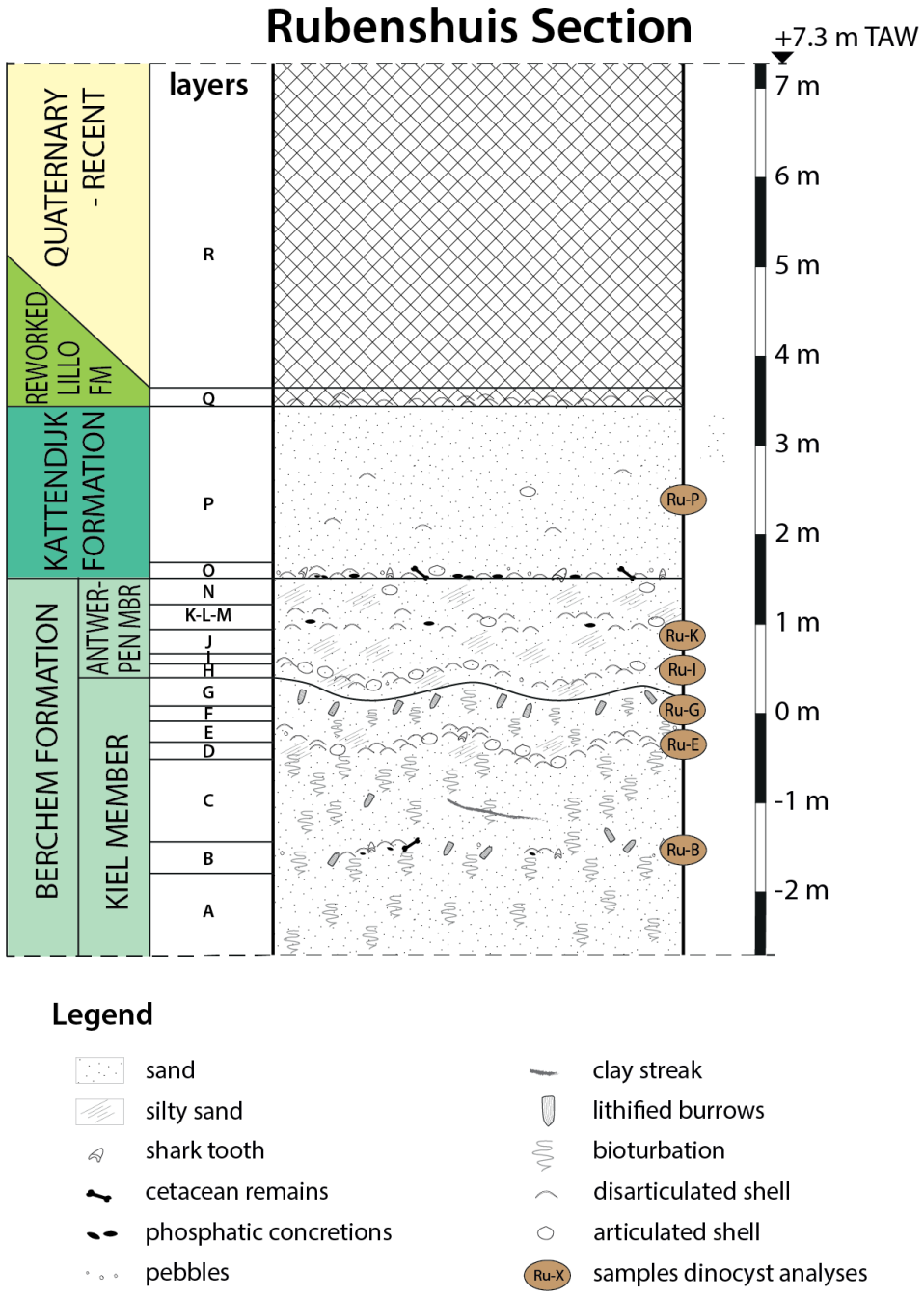

Figure 2. Lithology and lithostratigraphy at the Rubenshuis outcrop. The palynological sample locations are indicated. Depths are given in relation to the TAW reference level.

the definition of this member outlined by Louwye et al. (2023a).

The overlying layer H is characterised by dark green to blackish, fine-grained sand with more silt and some shells. It shows undulations due to load casting. Based on these characteristics, layer H is interpreted as the base of the Antwerpen Member, following Louwye et al. (2023b). The marked colour difference between both members, visible in dry profiles (Figs 3D & 3E), is in accordance with observations in temporary outcrops south and southeast of studied outcrop (Louwye et al., 2010; Hoedemakers & Dufraing, 2018; Everaert et al., 2019; 2020; De Schutter & Everaert, 2020; Louwye et al., 2023a). The overlying sediments, up to layer N, are also

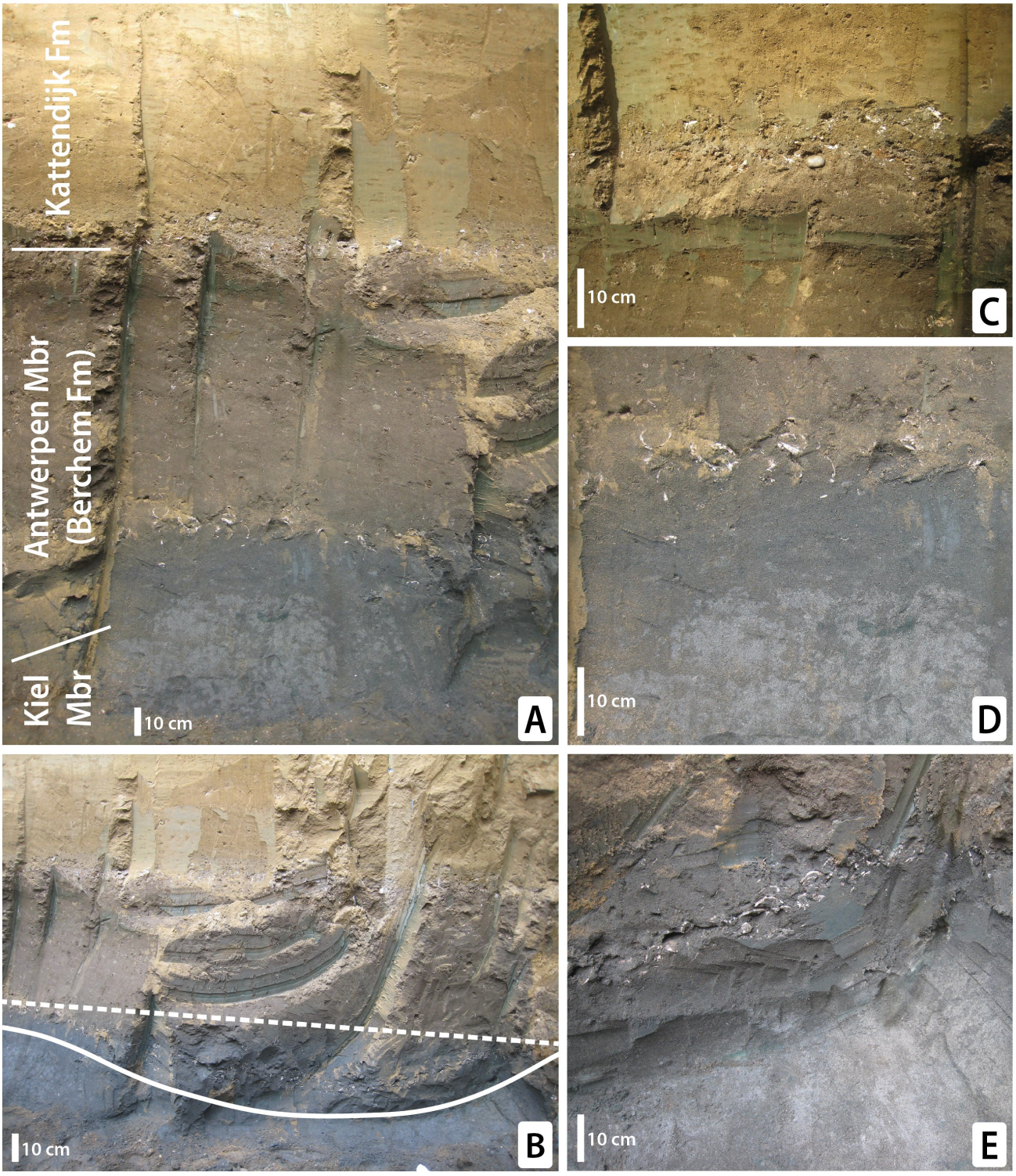

Figure 3. A. Cross-section of the Kattendijk Formation and exposed parts of the Berchem Formation (Kiel and Antwerpen members). **B.** Full line: undulating base of the Antwerpen Member due to load casting. Dashed line: straight base of the post-depositional oxidation front. **C.** Close-up of the basal gravel of the Kattendijk Formation (layer O). **D.** Detail of the boundary between the greyish Kiel Member (layer G) and the dark-coloured base of the Antwerpen Member (layer H). Above the basal shell bed of the Antwerpen Member (layer I), the sediment (layer J) is discoloured brown due to post-depositional oxidation. The top of the Kiel Member is somewhat disturbed by patches of dark sediment from the overlying Antwerpen Member, representing intense bioturbation and possibly attached and detached pseudonodules. **E.** Another view of the boundary between the Kiel and Antwerpen members, marked by a contrasting colour difference. The top of the greyish Kiel Member is exposed flat on the bottom surface. Photographs: July 6, 2022.

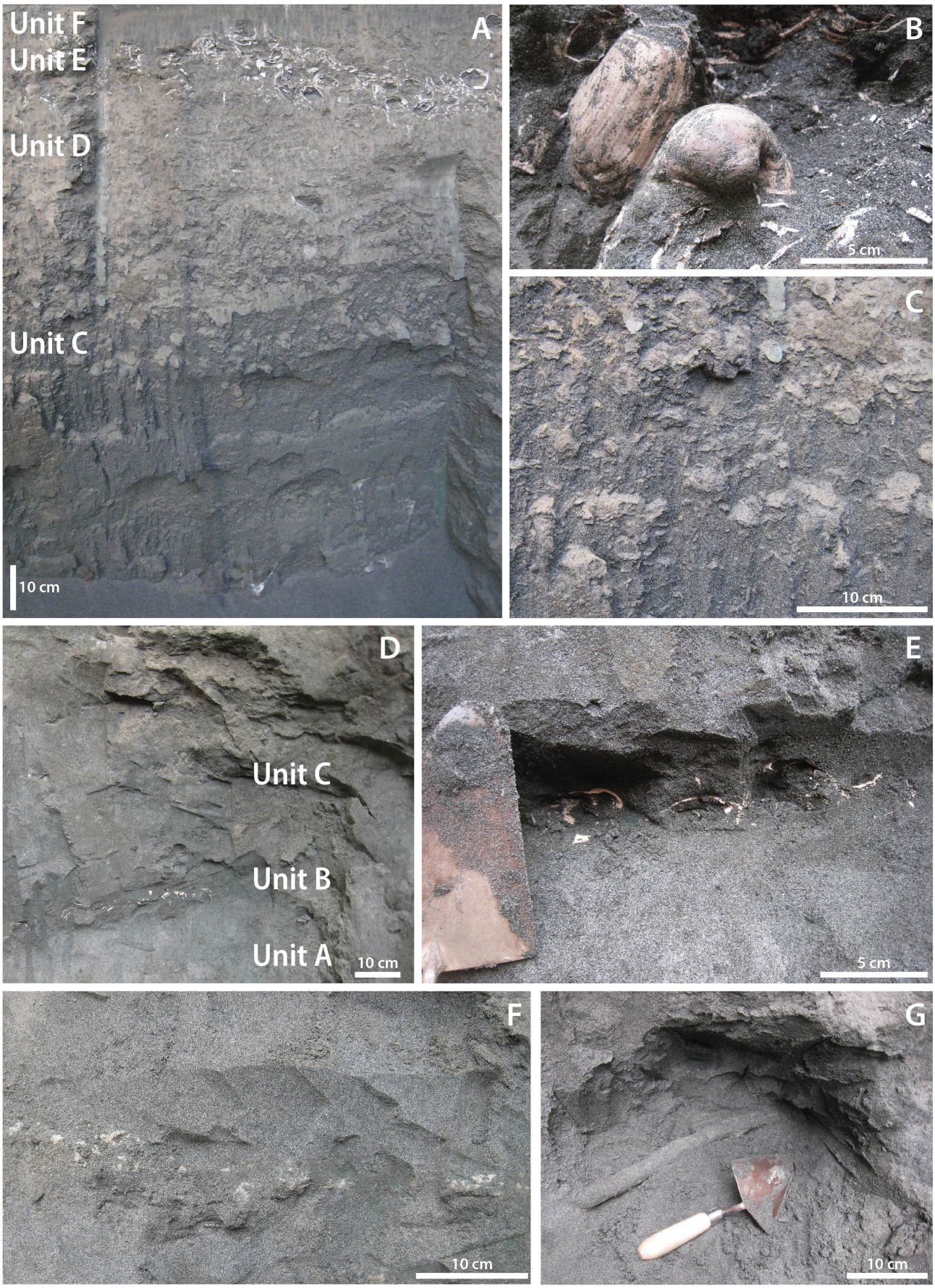

Figure 4. A. Transition of the silt-poor sand of layer C to the silty interval of layers D-E-F within the Kiel Member. **B.** Detail of the shell bed (layer E) in the silty interval. *Glossus lunulatus* cf. *lunulatus* (see Plate 1.4a–b) in the foreground, on the back left a large specimen of *Panopea kazakovae* in life position. **C.** Bioturbated sand within the top of layer C, including large cross-sections of *Ophiomorpha* and small *Macaronichnus segregatis* in between. **D.** Succession of layers A-C, layer B yields a small lens with very fragile shells. **E.** Detail of D. Partially decalcified valves of *Glycymeris obovata baldii*, generally in convex-up orientation. **F.** Clay streak within layer C. **G.** Lithified, subhorizontal burrow of *Ophiomorpha* in layer B. Photographs: August 16, 2022.

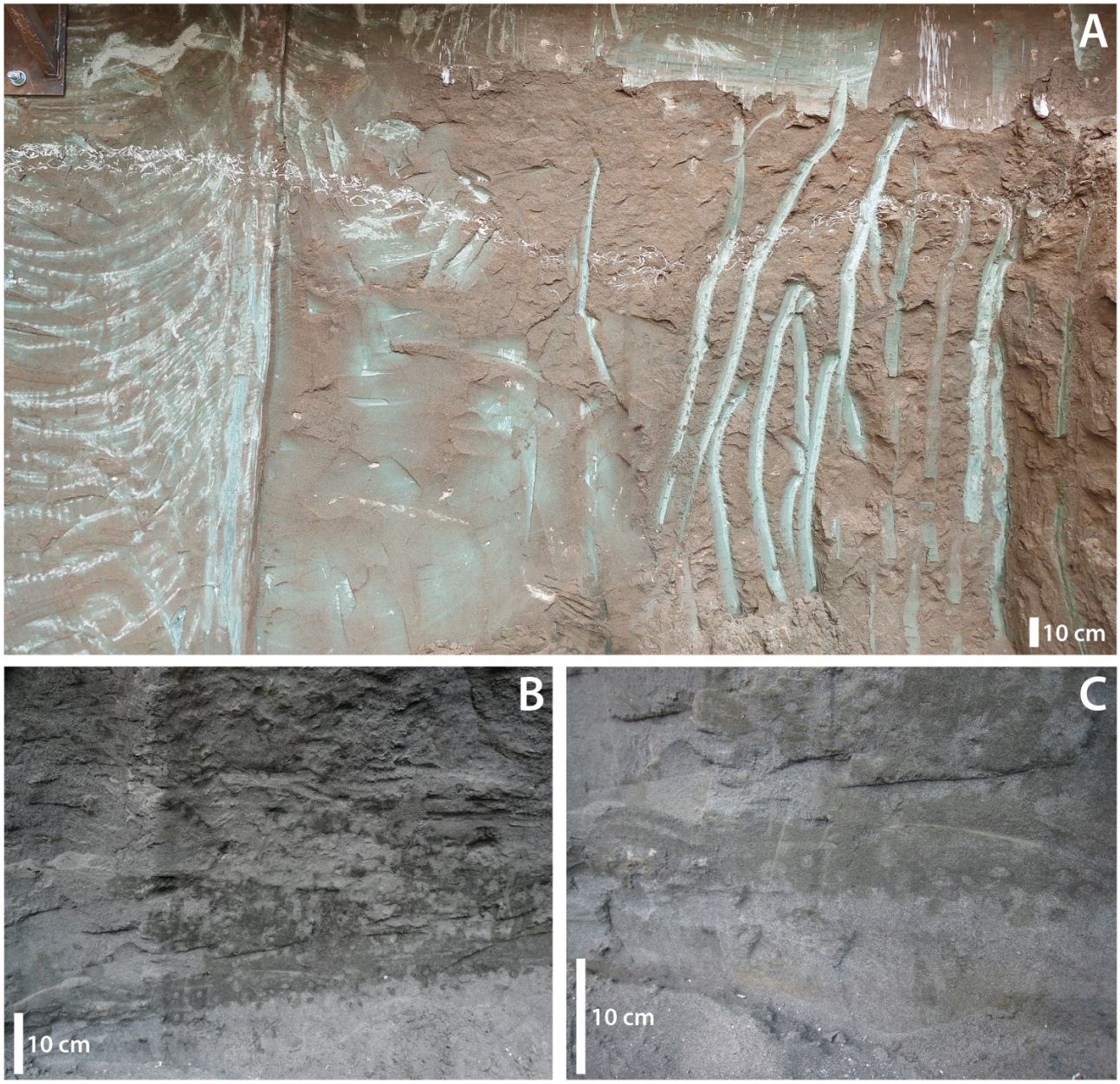

Figure 5. A. The upper part of the Kiel Member in the southern, cement hardened wall (hence the unnatural colours). The shell bed (layer E) is undulating and can be classified as a "simple load cast". **B.** Irregular distribution of silty (dark coloured) zones and silt-poor (grey) sand within the lower part of layer C (Kiel Member). **C.** Detail of B. Alternatively to bioturbation, circular patches on the interface of irregular sandy and silty zones may also be interpreted as attached and detached pseudonodules. Photographs: August 16, 2022.

attributed to the Antwerpen Member (Fig. 3A–B), representing a homogeneous interval of silty, fine-grained sand with relatively well-preserved molluscs, both dispersed and concentrated in shell beds (Louwye et al., 2023b). Compared to the underlying Kiel Member, the glauconite content (>63 µm) is reduced by up to 20% (Fig. 6).

Layers O-P are characterised by light ochre-coloured, glauconitic, fine-grained sand with dispersed shells. This interval represents the Kattendijk Formation (Fig. 3A; De Meuter & Laga, 1976; Deckers et al., 2023b). The glauconite content is within the 15–25% range, similar as reported by Laga (1972). The Kattendijk Formation is separated from the underlying Berchem Formation by a distinct transgressive basal gravel (layer O) which is highly fossiliferous (Fig. 3C).

The Kattendijk Formation is capped by another basal gravel, consisting of a dense accumulation of Pliocene shells (layer Q). It is probably a reworked remnant of the Lillo Formation. The highest part of the section (layer R) is disturbed by anthropogenic activity.

4.2. Sediment oxidation (diagenesis)

The sediments in the upper part of the outcrop (layers J to Q) generally have a relatively brown/ochre colour that grades to blackish and greyish towards the base of the outcrop (Fig. 3A). This brown/ochre discolouration is attributed to iron oxides-hydroxides around the sand grains and is indicative for post-depositional oxidation by groundwater lowering. In the current section, the straight base of the oxidation front lies above the undulating base (layer H) and basal shell bed (layer I) of the Antwerpen Member (Fig. 3B). Both layers still display their original dark green to black colour (Fig. 3D).

4.3. Soft-sediment deformation in the Berchem Formation

"Simple load casts" (sensu Owen, 2003) are known from the boundary between the Kiel and Antwerpen members, expressed as U- and V-shaped undulations (Everaert et al., 2019, 2020). Although less pronounced, they are also present in the

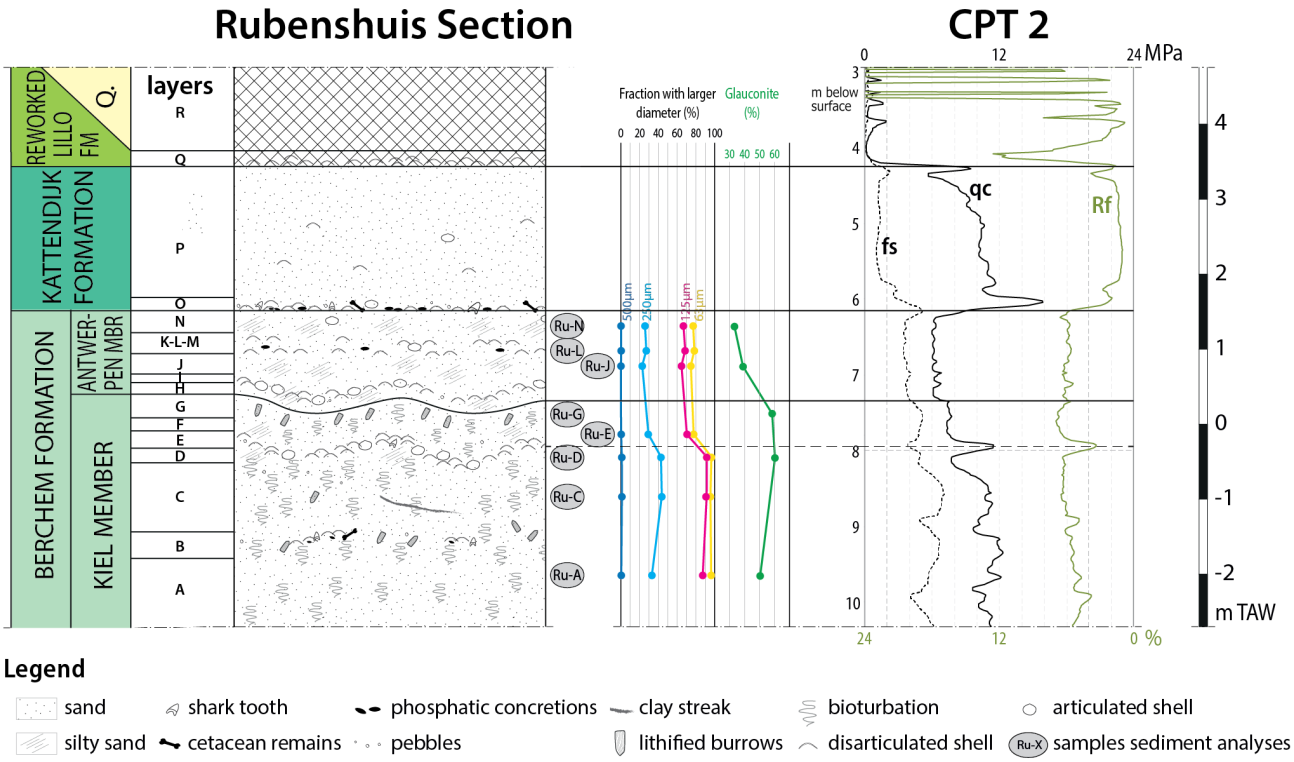

Figure 6. Correlation of the litholog with a Cone Penetration Test that was performed at the site before the excavation (CPT2 on the map of Fig. 7). Three classic CPT parameters are displayed: the cone resistance (qc), the sleeve friction (fs) and the friction ratio (Rf). Granulometric and glauconite analyses are taken from Deckers et al. (2023a).

Rubenshuis outcrop with wavelengths that span several metres and amplitudes up to 0.5 m (Fig. 3B). Above the basal shell bed of the Antwerpen Member (layer I), load casts are absent. Below the base (layer H), the shell bed (layer E) in the upper part of the Kiel Member (Fig. 5A) also displays pronounced undulations due to simple load casts.

While the boundary between the Kiel and Antwerpen members can be razor-sharp (Argenta, Post X and Posthofbrug outcrops; Hoedemakers & Dufraing, 2018; Everaert et al., 2019; 2020; De Schutter & Everaert, 2020), it is often somewhat blurred or disturbed in the Rubenshuis outcrop. In the top of the Kiel Member, irregularly dispersed patches with dark sediment of the overlying Antwerpen Member are observed (Fig. 3D). Many of these can be explained by burrowing activity during the onset of the deposition of the Antwerpen Member. Alternatively, some of these patches may be interpreted as smaller-scale liquefaction structures, similar to attached and detached pseudonodules (Owen, 2003). Comparable phenomena are observed deeper within the Kiel Member near layer B, as the base of a silty zone of layer C shows intermixing of circular patches of darker, silty sand from layer C and paler, silt-poor sand from Layer A (Fig. 5C). While bioturbation is abundant in the surrounding sediment, these patches may also be attached and detached pseudonodules from small pendulous load casts (compare with fig. 2b of Owen, 2003). However, a clear distinction with bioturbation cannot be made.

Irregular silty zones more than 30 cm thick are present within layer C, containing irregular spots with silt-poor sand (Fig. 5B). These zones transitioned laterally by sharp, irregular boundaries towards zones of sand with little to no silt. At the moment, no explanation exists for these features.

5. Geotechnics: Cone Penetration Tests

5.1. Standard parameters

Cone Penetration Tests have been used to characterise the Berchem and Kattendijk formations in the city of Antwerp (Deckers & Louwye, 2020; Deckers & Everaert, 2022). Major differences are known to exist between both formations: the Kattendijk Formation shows low and uniform friction ratios (Rf) of <2%, whereas the Berchem Formation shows generally high Rf of >4%, fluctuating up to 8% (below the depths shown in Fig. 6). In general, the Cone Resistance (qc) of the Kiel Member is about 12–14 MPa and 8 MPa in the Antwerpen Member (Deckers & Everaert, 2020; Deckers et al., 2023a). In the studied CPT 2 (Fig. 6), the values in the upper part of the Berchem Formation are slightly lower than usual, around 6 MPa for the Antwerpen Member and 10 to 14 MPa for the major part of the Kiel Member (14 MPa below the section shown in Fig. 6). Particularly, the top metre of the Kiel Member shows distinctly lower values, towards 8 MPa. Nevertheless, the characteristic, abrupt drop in qc values between the Kiel and Antwerpen members can still be observed. The Kattendijk Formation generally shows higher qc values of mostly >10 MPa, often >20 MPa. On CPT 2, qc values are about 11 MPa. Local qc spikes in the Kiel Member and Kattendijk Formation are correlative with the observed shell beds. The top section of CPT 2 shows very low qc values and strongly fluctuating Rf values, reflecting anthropogenic disturbance of the subsurface.

5.2. Soil Behaviour Type Index

From the standard CPT parameters, the Soil Behaviour Type (SBT) Index can be derived (Robertson, 1990). These curves can be indicative of grain-size trends, as shown for example in Schiltz (2020). Based on these trends, four major SBT

sequences can be noted within the Berchem Formation (Fig. 7), herein referred to as SBT sequences 1 to 4. For comparison with the various layers described in the field and grain-size analyses, see Figure 6.

The lowermost SBT sequence 1 with a fining upward (FU) trend runs from the bottom of the CPTs at 20 m below the surface up to 13 m and is therefore located below the exposed sediments at the Rubenshuis (Fig. 7). SBT sequence 1 is followed by SBT sequence 2 with a coarsening upward (CU) trend that ends between 9 and 10 m depth. This CU SBT sequence consists of up to 4 successive higher frequency CU SBT sequences that can be followed throughout the different CPTs (orange arrows on Fig. 7). The uppermost part of this SBT sequence 2 is correlative with the silt-poor, fine to medium fine sand of layer A that was observed at the basal part of the temporary outcrop. The coarsening upward SBT sequence 2 is possibly topped by the fossiliferous layer B, which is located at the base of the fining upward SBT sequence 3. As the layer B consists of small lenses with concentrations of heavier material, it might represent a (minor) lag deposit. In CPT2 and CPT3, fining upward SBT sequence 3 starts across layer C and ends up around the silty layer D. In CPT1, this fining upward SBT sequence is lacking. Also in field observations, layer C showed sharp, irregular lateral lithological changes from silt-poor to silty sand, so it is expected that this layer shows no uniform CPT signature across the outcrop. SBT sequence 3—if present—is topped by SBT sequence 4, which comprises numerous higher frequence sequences in the upper part of the Berchem Formation, however without significant overall fining or coarsening trends. SBT sequence 4 correlates with the uppermost part of the Kiel Member and the Antwerpen Member, which is consistent with the presence of a silty interval in the upper part of the Kiel Member, superficially resembling the lithology of the Antwerpen Member. The differences between the SBT sequence boundaries within the CPTs and the layers described in the field are probably also due to different locations of the CPTs compared to the studied parts of the temporary outcrop. Besides, the course of the CPT-derived sequences might also suggest sedimentary events like erosion and filling, causing lateral changing of sequences at short distances, which is an alternative explanation for the disappearing of sequence 3 in CPT1. However, these interpretations cannot be confirmed or disproven from the field observations.

6. Marine palynology

Samples Ru-B, Ru-E, Ru-G and Ru-I hold a moderate to poorly preserved dinoflagellate cyst assemblage (Table 2). Many specimens are fragmented most probably due to mechanical degradation. Samples Ru-K and Ru-P contain diverse and well-preserved dinoflagellate cyst assemblages.

The samples Ru-B and Ru-E of the Kiel Member (Fig. 2) can be placed within the DN2c subzone of de Verteuil & Norris (1997) defined as the interval from the highest occurrence (HO) of *Cordosphaeridium cantharellus* to the HO of *Exochosphaeridium insigne*. The key species *C. cantharellus* is absent while *E. insigne* is present. The DN2c has a middle Burdigalian age. Both samples Ru-B and Ru-E can also be correlated with the Danish *Exochosphaeridium insigne* Zone which has a calibrated age of 18.4 Ma to 17.8 Ma (middle Burdigalian) (Dybkjær & Piasecki, 2010).

The overlying samples Ru-G and Ru-I (Fig. 2) both hold quite similar dinoflagellate cysts associations, and the samples originate from the top of the Kiel Member and the basal shell bed of the Antwerpen Member, respectively. The marker *E. insigne* is absent in both samples. Both samples can be correlated to the *Cousteaudinium aubryae* Zone (DN3) of de Verteuil & Norris (1997), a 'gap' zone between the HO of *E. insigne* and the lowest occurrence of *Labyrinthodinium truncatum*. The DN3 zone is largely correlatable with the *C. aubryae* zone of Dybkjær & Piasecki (2010), a zone with a late Burdigalian age (17.8 Ma to 15.97 Ma). Ru-I was taken in the basal shell bed of the Antwerpen Member, a layer which has always been placed within the Langhian, as it holds the superjacent *L. truncatum* Zone. Hence, this result is unexpected. An overview of the stratigraphic assignments of the Antwerpen Member is given in Louwye et al. (2020a).

Sample Ru-K from the Antwerpen Member, taken 45 cm above sample Ru-I (Fig. 2), holds *Labyrinthodinium truncatum* and can be assigned to the *Distatodinium paradoxum* DN4 zone of de Verteuil & Norris (1996) and the early Langhian *Labyrinthodinium truncatum* zone of Dybkjær & Piasecki (2010). The latter zone has a calibrated age between 15.97 Ma to 14.8 Ma.

The highest sample Ru-P from the Kattendijk Formation (Fig. 2) contains a dinoflagellate cyst assemblage comparable to the assemblages recorded in the Pliocene Kattendijk Formation in the Deurganckdok outcrop near Doel (Louwye et al., 2004) and in the Tunnel-Canal Dock (De Schepper et al., 2009). Both outcrops are located in the greater Antwerp area (Fig. 1). The key species is *Operculodinium tegillatum* which has a range from 5.0 Ma to 4.7–4.4 Ma in Belgium (De Schepper & Head, 2008), and is restricted to the Zanclean Kattendijk Formation.

7. Macropalaeontology and biostratinomy

7.1. Berchem Formation – Kiel Member

The Kiel Member in the Rubenshuis section displayed two fossiliferous horizons (layers B and E, Fig. 2), separately discussed here.

Biostratinomy and taphonomy. Layer B (Fig. 4D–E) consists of local, small lenses with rounded pebbles/concretions (<2 cm), bioclasts and locally coarse quartz grains. These lenses are relatively enriched with fish remains, predominantly bones and teeth of teleosts, but also elasmobranch teeth. Compared to the surrounding sediment the enrichment indicates erosion and reworking, likely representing a minor lag deposit. Locally, thin concentrations of concordant disarticulated valves of *Glycymeris obovata baldii* occur, stacked in convex-up orientation (Fig. 4D–E). Stacked, convex-up shells are often associated with transported, storm-reworked concentrations and reorientation of shell debris by currents during the early stages of storms (Kidwell & Bosence, 1991; Norris, 1986). However, the excellent preservation of most shark teeth suggests that this highly energetic reworking was not very intensive or prolonged, and such preservation can be a trait of winnowed concentrations (Fürsich & Oschmann, 1993). The diagenetic, partial decalcification of the shells did not allow to determine the presence of *in situ* abrasion. The relatively continuous presence of lithified, branching *Ophiomorpha* confirms a low sedimentation rate with sufficient time to colonize the sea floor (Fig. 4G).

Layer E (Figs 4A, 5A) is a continuous, dense shell bed dominated by *Glycymeris obovata baldii*. Due to the abundant presence of both articulated and disarticulated *Glycymeris*, it might be considered as a "mixed autochthonous-parautochthonous assemblage" (sensu Kidwell et al., 1986). Autochthonous elements include a *Panopea* observed in life-position (Fig. 4B) and numerous articulated *Glycymeris*. Stacked, disarticulated valves of *Glycymeris* can be considered parautochthonous. In general, the shells are fairly well preserved with little fragmentation, which argues against a long-term

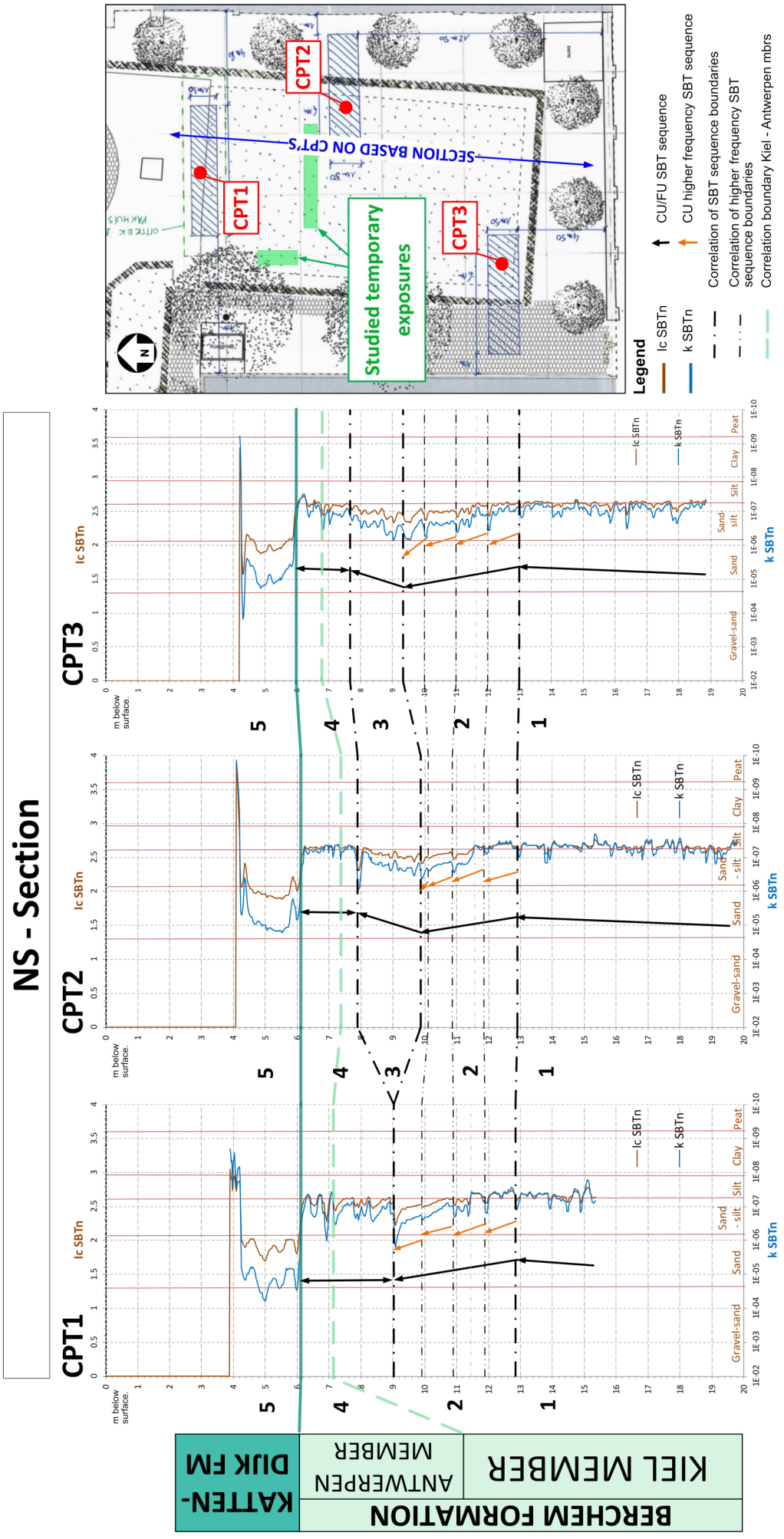

Figure 7. Soil Behaviour Type (SBT) Index (see Schiltz, 2020) throughout the Rubenshuis outcrop. Derived normalised hydraulic conductivity (k SBTn) and normalised soil behaviour type index (Ic SBTn) values are given. Geotechnical SBT-sequences are indicated by numbers and separated by dashed, bold black lines. The black arrows indicate trends in grain sizes (coarsening up or fining up). The fine black lines and the orange arrows indicate higher frequency SBT sequences. The green dashed line indicates the approximate position of the boundary between the Kiel and Antwerpen members, positioned at the characteristic drop in qc values observed before conversion to the SBT parameters. The geographical positions of the CPTs are indicated on a small map of the site. Depths are given in metres below the surface. CU = coarsening upward, FU = fining upward.

Table 2. Distribution of dinoflagellate cysts and other palynomorphs from the Rubenshuis outcrop. Raw numbers are given. See Fig. 2 for samples locations. *E.* = *Exochosphaeridium, C.* = *Cousteaudinium, L. tru.* = *Labyrinthodinium truncatum.*

Sample no.	Ru-B	Ru-E	Ru-G	Ru-I	Ru-K	Ru-P
Dinoflagellate cysts biozones Dybkjaer & Piasecki (2010)	*E. insigne* Zone		*C. aubryae* Zone		*L. tru.* Zone	-
Dinoflagellate cysts biozones de Verteuil & Norris (1997)	DN2c		DN3		DN4	-
Dinoflagellate cysts						
Achomosphaera andalousiensis subsp. *andalousiensis*						6
Achomosphaera andalousiensis subsp. *suttonensis*						1
Apteodinium spiridoides	14	9	9	3		
Ataxiodinium zevenboomii						3
Barssidinium graminosum						2
Barssidinium pliocenicum						3
Batiacaphaera minuta	11	6	12	5	4	4
Batiacaphaera sphaerica				2	2	
Bitectodinium tepikiensis					1	1
Cleistosphaeridium placacanthum	63	48	39	72	61	
Cordosphaeridium minimum					1	
Cousteaudinium aubryae	2	3	1	2	3	
Cribroperidinium tenuitabulatum			4	1	1	
Dapsillidinium pseudocolligerum			3	2	2	
Dinopterygium cladoides	1		3	1	3	
Distatodinium paradoxum		2	4	1	5	
Exochosphaeridium insigne	1	3				
Filisphaera microornata					1	
Heteraulacacysta campanula				4	4	20
Hystrichokolpoma rigaudiae			1	3	7	
Homotryblium spp. ind.		4	3			
Hystrichosphaeropsis obscura				2	1	
Impagidinium spp. ind.						5
Labyrinthodinium truncatum					2	
Lejeunecysta mariae	1		1			
Lejeunecysta psuchra						1
Lejeunecysta sp. ind.					1	
Lingulodinium machaerophorum	4	8	8	14	7	8
Melistasphaeridium choanophorum	7	1	2	7	4	3
Operculodinium? *borgerholtense*					1	
Operculodinium centrocarpum	5	3	3	5	3	120
Operculodinium centrocarpum sensu Wall & Dale						3
Operculodinium? *eirikianum*			1	1	2	
Operculodinium israelianum	1				2	13
Operculodinium longispinigerum			1			
Operculodinium piaseckii				1	3	
Operculodinium tegillatum						4
Palaeocystodinium golzowense			1	1	1	
Pentadinium laticinctum					1	
Polysphaeridium zoharyi	1	1				
Pyxidinopsis sp. ind.						
Quinquecuspis concreta		1		1	2	
Round Brown Cysts	3	1	2		3	
Reticulatosphaera actinocoronata	2	5	3	1	5	1
Selenopemphix brevispinosa		1		2	1	2
Selenopemphix indentata					1	
Selenopemphix nephroides	1	3	1	3	8	
Selenopemphix quanta						1
Spiniferites spp. ind.	115	96	85	136	118	78
Sumatradinium druggii	2	2		4	1	
Sumatradinium hamulatum	1			1		
Sumatradinium soucouyantiae	1		2		1	
Tectatodinium pellitum			1	2	2	3
Trinovantedinium ferugnomatum					1	
Trinovantdinium? *xylochophorum*					1	
Trinovantedinium sp. ind.	1	1			2	
Tuberculodinium vancampoae			1	1	1	
Reworked dinocysts	5	8	1	5	1	3
Acritarchs						
Cyclopsiella granosa/elliptica					2	
Cyclopsiella trematophora						2
Paraleciella indentata	6	9	14	3	4	2
Quadrina condita			1			
Small spiny acritarch	2			6	1	
Pollen (plants)						
Bisaccate pollen	96	46	89	79	19	61
Green algae						
Pterospermella sp. ind.				1		
Tasmanites sp. ind.		1	1		1	
Palynomorphs counted	346	262	297	372	298	350

"current concentration" as defined by Fürsich & Oschmann (1993). The frequent presence of stacked disarticulated valves of *Glycymeris* in a convex-up position shows the influence of repeated storm concentration events (Kidwell & Bosence, 1991). The final biofabric might be a relict element of a proximal tempestite, based on the biostratinomic characteristics of the shells outlined by Fürsich & Oschmann (1993). However, besides the sharp base of the shell concentration, no sedimentary structures (e.g. hummocky cross-stratification) have been observed that can support this interpretation. If such structures were present at all, they were erased by burrowing organisms that disturbed the sediment. The abundant presence of barnacles, often present within the articulated specimens (Plate 1.1), indicates that the shell communities were exposed for a prolonged period (Kidwell, 1989), possibly in a regime of reduced sediment supply (Kondo et al., 1998). Compared to layer B, less vigorous reworking and erosion is emphasised by the much lower number of pebbles, shark teeth and bones. Borings of polychaetes on the shells are conspicuously absent, in contrast to other shell beds in the Kiel Member (Everaert et al., 2020). The presence of coarser sand in articulated *Glycymeris* possibly results from exhumation and transport of articulated shells that were buried elsewhere.

Palaeontology. When compared to the faunas figured in Everaert et al. (2019), the palaeontological content of layer B is typical of the Kiel Member (Table 3). Aragonitic shells could not be collected as they were too fragile due to partial decalcification. Shark teeth are common (Plate 1.7–8), in addition to skeletal remains of teleost fishes and some cetacean bone fragments. In contrast to layer B, the fauna of layer E is dominated by well-preserved *Glycymeris* (Plate 1.1–2) and other shells (Table 3). The most common gastropod is *Ptychidia eryna* (before known as *Haustator eryna* or *Turritella eryna*, see also Harzhauser & Landau, 2019). The fossil content of layer E shows subtle differences with the faunas known from the "typical" Kiel Member (Argenta and Deurganckdok outcrops, coll. RBINS; Kievitstraat/Ploegstraat outcrop; coll. NBC).

In the Miocene of the North Sea Basin, a complex and little-

	Layer B	Layer E
Bivalvia		
Ennucula haesendoncki haesendoncki (Nyst & Westendorp, 1839)		2
Glycymeris obovata baldii Glibert & Van de Poel, 1965	x	15 + 3 art
Limopsis/Aspalima indet.		1
Pseudamussium lilli (Pusch, 1837)		2
Astarte radiata Nyst & Westendorp, 1839		2
Astarte cf. *convexior* Anderson, 1959		4
Astarte goldfussi Hinsch, 1952		2
Goodallia waeli (Glibert, 1945)		1
Erycinella chavani (Glibert, 1945)		1
Cyrtodaria angusta (Nyst & Westendorp, 1839)		8
Spisula aff. *subtruncata* (Da Costa, 1778)		7
Venus multilamella (Lamarck, 1818) s.l.		3
Cordiopsis polytropa nysti (d'Orbigny, 1852)	?	5
Arctica islandica (Linnaeus, 1767)	?	1
Glossus lunulatus cf. *lunulatus* (Nyst, 1835)		1
Glossus indet.	1	
Gastropoda		
Ptychidia eryna (d'Orbigny, 1852)		3
Euspira spp.		3
Gastropoda indet. - phosphatic casts		2
Scapophoda		
Dentalium spp.		3
Scapophoda indet.		1
Bryozoa		
Cupuladria/Reussirella spp.		7
Echinoidea		
Echinoidea indet. - spines	1	8
Cirripedia		
Actinobalanus collinsi Zullo & Perreault, 1989 - plate fragments	10	Ca. 300
Polychaeta		
Polychaeta indet. - scolecodonts	2	
Plantae		
Magnoliaceae indet.	1	
Elasmobranchii		
Carcharias gustrowensis (Winkler, 1875)	2	
Araloselachus vorax (Le Hon, 1871)	3	
Carcharhinus priscus (Agassiz, 1843)	1	
Notorynchus primigenius (Agassiz, 1835)	1	
Squatina sp.	3	3
Keasius rhenanus Reinecke, Von Der Hocht & Dufraing, 2015 - gill rakers	3	1
Selachii indet. - tooth fragments	7	
Raja holsatica Reinecke, Von Der Hocht & Gürs, 2008	5	
Raja indet. - thorn		1
Teleostei		
Trisopterus sculptus (Koken, 1891)		10
Teleostei indet. - skeletal fragments/teeth	Ca. 100	Ca. 150
Cetacea		
Odontoceti indet - rib fragment	1	
Reptilia		
Cheloniidae indet. - plate fragment ?	1	
Ichnofossils		
Ophiomorpha nodosa Lundgren, 1891 - lithified burrows	10	

Table 3. Macrofossils found in the Kiel Member (layers B and E) of the Berchem Formation. The specimens are housed in the RBINS collection (IG 34663). art = articulated specimens, x = present, but not in collection.

understood lineage of *Ennucula* occurs (Stein et al., 2016, as "*Leionucula*"). While *Ennucula haesendoncki haesendoncki* is restricted to the Langhian Antwerpen and Zonderschot members, *Ennucula haesendoncki hanseata* is dominant in the Burdigalian Edegem Member (Ringelé, 1974; Janssen, 1984). Until now, only *E. h. hanseata* was known from the Kiel Member: one specimen has been described from the Deurganckdok Sandstone Bed by Herman & Marquet (2007), while multiple specimens were recently collected from the Kiel Member in the Royerssluis temporary outcrop (unpublished data SE, 2024). *E. h. hanseata* also occurs in the German upper Burdigalian "Unteren Glimmerfeinsand Formation" of Werder (Germany; Stein et al., 2016), the Dutch upper Burdigalian to lower Langhian Miste bed (Janssen et al., 1984; Munsterman et al., 2024) and the Dutch Langhian to early Serravallian Stemerdink Member (Janse & Janssen, 1983; Munsterman et al., 2024). Due to the concave "depression" of the anterior teeth row, which does not converge with the dorsal margin (Plate 1.5a–b), two fragments from layer E in the Rubenshuis section are closer to *E. h. haesendoncki*. Besides, two better preserved specimens of *E. h. haesendoncki* were encountered in 2023 in the Kiel Member in a PIPDA borehole in Kapellen (DOV 1434-B-G227574-9_Kapellen3_WVP27; M_ID 5068; depth 80 m) (Plate 1.6a–b). Hence, based on the dinocyst dating of layer E (*Exochosphaeridium insigne* zone) and the range of the intermediate *Cousteaudinium aubryae* zone (Dybkjær & Piasecki, 2010), the first occurrence of *Ennucula haesendoncki haesendoncki* in the Antwerp region appears at least 1.8 Ma earlier than previously assumed. Despite these new findings, the taxonomic and evolutionary relationship of both subspecies remains an open question.

In the past, Glossidae have often been used as biostratigraphic tool in the Neogene of Belgium (Herman & Marquet, 2007). While *Glossus lunulatus crassus* and *Glossus burdigalensis cypriniformis* are both present in the Edegem Member (Glibert, 1945; Louwye et al., 2010; coll. NBC), the former disappears and the latter continues in the overlying Kiel Member (Herman & Marquet, 2007; Everaert et al., 2020). However, a large specimen collected from layer E is very different from *G. b. cypriniformis* due to its protruding umbo, few strong plicae and overall tumid shape (Plate 1.4a–b). At the same time, its umbo and plicae are too weak to allow identification as *G. l. crassus*. Hence, it is more similar to *G. l. lunulatus* from the Antwerpen Member (Plate 2.3, see also plate 3.2 in Everaert et al., 2020), although subtle morphological differences exist (e.g. the more rounded ventral margin in RBINS 7740). For now, we tentatively assign this specimen to *Glossus lunulatus* cf. *lunulatus*. Similar tumid valves are abundant in the clayey Berchem Formation at Rumst/Terhagen, displaying a considerable morphological variation (coll. NBC, Leiden). These sediments are coeval to layer E (middle Burdigalian; Louwye, 2005 and Louwye & Munsterman, pers. comm. 2022). More recently, many fragments of similar specimens were collected from a bed with stacked *Glycymeris* in the Kiel Member at the Royerssluis temporary outcrop (unpublished data SE, 2024). Unlike layer E, the facies of this shell bed was very similar to that described by Everaert et al. (2020) from the Argenta outcrop.

Hundreds of mostly disarticulated barnacles were encountered within valves of *Glycymeris* in Rubenshuis layer E (Plate 1.1). In the Argenta section, these were found attached on *Glycymeris obovata baldii* in life position (Everaert et al., 2020, plate 1). At the time, these barnacles were tentatively identified as *Balanus* (s.s.) aff. *stellaris* (Brocchi, 1814). However, comparison of the general shape of the plates and the depicted terga and scuta (Everaert et al., 2020, plate 1.5A–B) allows a re-identification as *Actinobalanus collinsi* (pers. comm. Perreault, 2023) described from the Edegem Member by Zullo & Perreault (1989).

7.2. Berchem Formation - Antwerpen Member

The Antwerpen Member holds multiple fossiliferous levels. Layer I can be interpreted as the so-called 'basal shell bed' discussed in Everaert et al. (2020). Therefore, only layers K and M are discussed here.

Biostratinomy and taphonomy. The matrix-supported accumulations in layers K and M are dominated by thin and small shells (Plate 2.4) and hold less *Glycymeris obovata baldii*. The shell accumulations are uncrowded and vaguely delimited (Fig. 3A, centre of the Antwerpen Member). Both articulated and disarticulated bivalves occur in different orientations, but always concordant with bedding. These characteristics may indicate gradual biogenic accumulation on a calm seabed with less influence from currents and/or storms than the surrounding shell concentrations. Quiet conditions are confirmed by the coral *Flabellum tuberculatum* (Plate 2.1). After being covered by layer (N), the stable seabed was colonised by deeply burrowing *Panopea*, occurring in life-position (Plate 2.2).

Palaeontology. All species are typical of the Antwerpen Member (Table 4) and the presence of *Ptychidia eryna* (Table 4) is characteristic of the lower part (see Deckers et al., 2023a) of the Antwerpen Member (Marquet, 1991; Louwye et al., 2010; Everaert et al., 2020). Higher in this member, it is replaced by *Oligodia spirata* (before known as *Turritella subangulata*, see Harzhauser & Landau, 2019) which was found reworked in the base of the Kattendijk Formation.

7.3. Kattendijk Formation

The majority of the fossils has been collected in the basal gravel of the Kattendijk Formation (layer O) (Fig. 3C). A similar shelly fauna was found dispersed in the overlying layer P. The absence of sedimentologic shell concentrations and scour structures in layer P suggests a fairly continuous background sedimentation without significant reworking events.

Biostratinomy and taphonomy. Layer O has an erosive base and represents a transgressive lag deposit, containing rounded

Table 4. Macrofossils found in the Antwerpen Member (layers K-L-M) of the Berchem Formation. The specimens are housed in the RBINS collection (IG 34663). art = articulated specimens, x = present, not in collection.

	Layers K-L-M
Bivalvia	
Ennucula h. haesendoncki (Nyst & Westendorp, 1839)	1
Pseudamussium lilli (Pusch, 1837)	x
Aspalima decussata (Nyst & Westendorp, 1839)	1
Korobkovia woodi (Nyst, 1861)	3
Diplodonta rotundata (Montagu, 1803)	2
Spisula aff. *subtruncata* (Da Costa, 1778)	x
Glossus lunulatus lunulatus (Nyst, 1835)	1 + 1 art
Venus multilamella multilamella (Lamarck, 1818)	1
Panopea kazakovae Glibert & Van de Poel, 1966	2 art
Gastropoda	
Ptychidia eryna (d'Orbigny, 1852)	x
Echinophoria cf. *bicoronata* (Beyrich, 1854)	x
Scleractinia	
Flabellum tuberculatum Keferstein, 1857	2
Echinoidea	
Echinoidea indet. - spines	2

phosphatic concretions, pebbles, sandstones, and closely packed bioclasts (Fig. 3C). The rounded clasts indicate reworking and a prolonged residence time on the sea floor, resulting in mechanical degradation. In contrast, most shells are well preserved without significant abrasion, contrary to the features one might expect in a basal gravel. Several taxa derived from the underlying Antwerpen Member do not show clear signs of reworking (*Glycymeris obovata baldii*, *Venus multilamella multilamella*, *Astarte radiata*, *Mimachlamys angelonii*, *Oligodia spirata*, *Reussirella/Cupiladria*, large echinoid spines). While large parts of the Antwerpen Member were eroded, these taxa were apparently only reworked with little abrasion. The Lower Pliocene shells are regularly affected by bioerosion (including *Maeandropolydora*) and also articulated specimens occur, proving an *in situ* colonization by infauna (*Lucinoma borealis*, *Astarte corbuloides*, *Laevastarte ariejansseni* and *L. omalii omalii*).

Palaeontology. A total of 27 bivalve and eight gastropod species have been recorded, of which at least four bivalve and one gastropod species were certainly reworked from the underlying Middle Miocene (Table 5, see Plate 3). Vertebrate remains were also found, including whale vertebrae and both well-preserved and worn shark teeth.

The thickest successions of the Kattendijk Formation are present northwest of Antwerp (Deckers & Louwye, 2020). Especially near Doel and Kallo, 10–15 km (north)west of the Rubenshuis outcrop, the molluscs of these successions have been studied in detail (Marquet, 1998, 2002, 2004, 2005). While only 33.3% of the autochthonous bivalves and gastropods from layer O occur in the lowermost part of the Kattendijk Formation in Doel and Kallo, 90.0% of the species in layer O also occur in the "*Petaloconchus* horizon" (Table 5; reworked species not included). The latter horizon is a small "reef" mainly composed of the gastropod *Petaloconchus intortus*, encountered at multiple localities in Doel and Kallo between 2.0 and 3.75 m above the base of the Kattendijk Formation (Herman et al., 1974; Marquet, 1984; Vervoenen, 1995; Goolaerts, 2000). The development of this reef occurred during a steady, well-oxygenated period of non-deposition, and was abruptly terminated by a high-energy event (probably a storm) (Vervoenen, 1995; Goolaerts, 2000; Marquet & Herman, 2009). The absence of *Petaloconchus* in the Rubenshuis outcrop testifies to different environmental conditions. Given that these vermetid colonies mostly live in a very narrow belt, making them useful as Biological Sea-Level Indicators (Schiaparelli et al., 2006), the water depth might have been unfavourable. However, Vescogni et al. (2008) found that extinct *Petaloconchus* have a wider palaeobathymetric range than recent vermetids (e.g. *Dendropoma*), namely from the upper subtidal zone to 30–50 m depth. Therefore, other factors such as higher exposure to waves or stronger bottom currents should also be considered. Besides, some other species, largely restricted to the *Petaloconchus* horizon, are also missing in the Rubenshuis outcrop (e.g., *Turritellinella vanderfeeni*, *Verticordia cardiiformis*; Marquet, 1998; 2005). Contrarily, colonies of *Ditrupa*, typical of layer O, are absent from the *Petaloconchus* horizon. In the Mediterranean, high densities of *Ditrupa arietina* have been found predominantly at depths between 20 and 30 m in well-sorted fine and muddy sand (Grémare et al., 1998; Hartley, 2014). This is slightly shallower than the 45–55 m depth inferred by Marquet (2004) for the Kattendijk Formation at Doel and Kallo.

In contrast to the lower part of the Kattendijk Formation in Doel and Kallo, 95.7% of the autochthonous species in layer O also occur in the Pliocene bivalve fauna in sample I00 6+7 of Ringelé (1974) (Table 5). This sample was taken from the highest fossiliferous level of the Kattendijk Formation in the temporary "Oosterweel" outcrop (Fig. 8) at the junction between the 5th Havendok and the Amerikadok, about 3.9 km NNW of the Rubenshuis outcrop (Laga, 1972; Fig. 1). This level, not observed in Kallo and Doel, was characterised by large numbers of *Ditrupa* and the presence *Pygocardia rustica tumida* forma *solida*. This is also the case in layer O of the Rubenshuis outcrop (Plate 3.8a–b). In the Antwerp area, various forms and subspecies of *Pygocardia rustica* are restricted to specific stratigraphic intervals in the Kattendijk and Lillo formations. It remains debated to what extent these morphological traits reflect evolution and/or local ecophenotypic variation (Bosch & Wesselingh, 2006). However, the forma *solida* has only been found *in situ* in the highest part of the Kattendijk Formation in temporary outcrops on the right bank of the Scheldt River (Ringelé, 1974; Janssen et al., 1984; Marquet, 2005) and a temporary outcrop in Melsele (Marquet, 2005). In Kallo and Doel, this part of the Kattendijk Formation is missing and the forma *solida* only occurs reworked in the Luchtbal Member or the basal gravel of the Oorderen Member (both Lillo Formation) (Marquet, 2005).

Another unusual observation is the common occurrence of *Laevastarte ariejansseni* in layer O. While this species is scarce in the Kattendijk Formation near Kallo and Doel, it becomes very common in the younger Luchtbal Member (Lillo Formation) (Marquet, 2005).

Two species of *Scalaricardita* are recognised in layer O. This genus was formerly included in the genus *Cyclocardia*, which recently appeared to be a non-monophyletic wastebasket taxon (Pérez & Giachetti, 2020). One specimen can be assigned to the earliest type of *Scalaricadita chamaeformis* (Sowerby, 1825), referred to as forma *orbicularis* by Janssen & Moerdijk (2004) (Plate 3.4a–b). *Scalaricardita scalaris* is very common and dominated by the inflated "early" form with coarse ribs

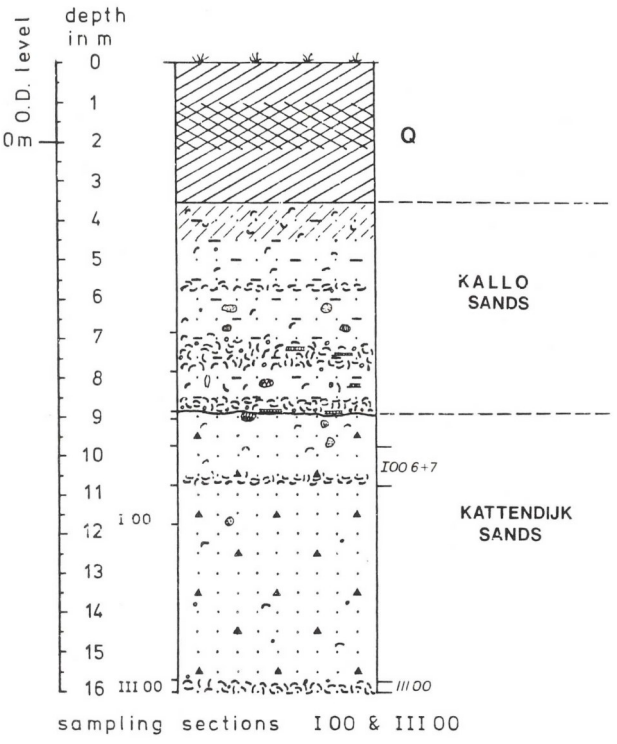

Figure 8. Oosterweel section described by Laga (1972), refigured after Ringelé (1974, fig. 4). The shell bed with numerous *Ditrupa* and *Pygocardia rustica tumida* forma *solida* is indicated as I00 6 + 7. The "Kallo Sands" are now attributed to the Oorderen Member (Lillo Formation), while the "Kattendijk Sands" represent the Kattendijk Formation.

Table 5. Macrofossils found in the base of the Kattendijk Formation (layer O). The specimens are housed in the RBINS collection (IG 34663). The stratigraphic distribution of molluscs in the Kattendijk and Lillo formations at Doel and Kallo follows Marquet (1998, 2002, 2004, 2005), the distribution of teleost otoliths follows Hoedemakers (2013). The records of Ringelé (1974) in the highest shell bed (I00) of the Kattendijk Formation in the Oosterweel outcrop are also provided. VR = very scarce, R = rare, C = common, N = numerous, x = present but abundance unknown, ? = presence unknown, fr. = fragments only, art = articulated specimens, RW = reworked from the Antwerpen Member. Other ID = Some species were attributed to other (incorrect or invalid) species by Ringelé (1974), these are *Aequipecten radians* (as *Lyropecten opercularis*), *Spaniorinus ambiguus* (as *Spaniorinus cimbricus*), *Scalaricardita chamaeformis* and *S. scalaris* (as *Cyclocardia triforma triforma*), *Laevastarte ariejansseni* (included within *Astarte omalii omalii*) and *Ensis hausmanni* (as *Ensis* sp.). * Following Janssen (2014), *Limopsis anomala coxi* is here considered a subspecies of *Aspalima decussata*. ** For *Scalaricardita*, taxonomy follows Janssen & Moerdijk (2004) and Moerdijk et al. (2010). *Cyclocardia orbicularis orbicularis* as described by Marquet (2005) is reinterpreted as *S. scalaris* - Type 1 and *S. chamaeformis* forma *orbicularis.* *** Moerdijk et al. (2010) distinguished a second species within Marquet's *Abra prismatica*. For its distribution, the occurrences of *A. prismatica* are tentatively copied with '?'. **** Pouwer & Rijken (2022) reidentified *Euspira catena* of Marquet (1998) as *Euspira catenoides*.

		Kallo & Doel						Oosterweel
	Rubenshuis Layer 0	Kattendijk Fm (lower part)	Kattendijk Fm (*Petaloconchus*)	Luchtbal Member (Lillo Fm)	Oorderen Member (Lillo Fm)	Kruisschans Member (Lillo Fm)	Merksem Member (Lillo Fm)	Kattendijk Fm (highest bed, I00)
Bivalvia								
Yoldia semistriata (Wood, 1840)	3	VR	VR	VR	VR-C			x
Aspalima decussata coxi (Glibert & Van de Poel, 1965) *	8	VR	C	C				x
Glycymeris obovata baldii Glibert & Van de Poel, 1965	4RW							
Aequipecten radians (Nyst & Westendorp, 1839)	5	C	C	R				Other ID
Mimachlamys angelonii (De Stefani & Pantanelli, 1878)	1RW							
Lucinoma borealis (Linnaeus, 1767)	3 + 1 art	C	N	N	N	C		x
Spaniorinus ambiguus (Nyst & Westendorp, 1839)	1		VR	VR	VR-C			Other ID
Scalaricardita chamaeformis (Sowerby, 1825) forma *orbicularis* **	1		x	x				Other ID
Scalaricardita scalaris (Sowerby, 1825) - Type 1 **	8		x	x				Other ID
Scalaricardita scalaris (Sowerby, 1825) - Type 2	1			C	C	R		Other ID
Laevastarte omalii omalii (De la Jonkaire, 1823)	4 + 2 art		N	N				x
Laevastarte ariejansseni (Marquet, 2005)	8 + 1 art		R	N				Other ID
Astarte corbuloides De la Jonkaire, 1823	11 + 1 art		C	C				x
Astarte radiata Nyst & Westendorp, 1839	1RW							
Digitariopsis obliquata burtinea (De la Jonkaire, 1823)	4		C					x
Digitaria excurrens (Wood, 1853)	2		C	R				
Digitaria digitaria (Linnaeus, 1758)	3		C	C	C	C		x
Ensis hausmanni (Goldfuss, 1841)	1		R	*fr.*	R-C			Other ID
Abra prismatica (Montagu, 1808)	1		N	C	R			x
Abra spec. 1 *sensu* Moerdijk et al., 2010 ***	1		?	?	?			?
Arctica islandica (Linnaeus, 1767)	1	R	R	R	C	C		x
Pygocardia rustica tumida (Nyst, 1836) *s.l.*	2	x	?					x
Pygocardia rustica tumida (Nyst, 1836) forma *solida*	2							x
Venus multilamella multilamella Lamarck, 1818	1RW							
Varicorbula gibba (Olivi, 1792)	2	C	N	N	N	N	N	x
Hiatella arctica (Linnaeus, 1767)	1	C	N	C	C-N	C	C	x
Cyrtodaria angusta (Nyst & Westendorp, 1839)	1	R	R	R	N	R		x
Gastropoda								
Solariella maculata Wood, 1842	1		C		VR			
Turritellinella tricarinata tricarinata auct., (non Brocchi, 1814)	3	VR			C	R		
Oligodia cf. *spirata* (Brocchi, 1814)	1RW							
Euspira cf. *catenoides* (Wood, 1842) ****	4		R	R	C	R		No data
Euspira cf. *hemiclausa* (Sowerby, 1824)	1?		R		C-N	R		
Epitonium subulatum (Sowerby, 1823)	1		C					
Ringicula buccinea (Brocchi, 1814)	4		C	R				
Cylichna cylindracea (Pennant, 1777)	3		R	R	R-N	R		
Scapophoda								
Dentalium aff. *dumasi* (Cossmann & Peyrot, 1916)	2RW?		?					No data
Dentalium sp.	1		?					
Brachiopoda								
Glottidia dumortieri (Nyst, 1843)	3	?	x	?	x	?	?	No data
Polychaeta								
Ditrupa arietina (Müller, 1776)	32		x	x	x	?	?	N
Cirripedia								
Balanidae indet.	4	x	x	x	x	x	x	No data
Bryozoa								
Reussirella/Cupuladria indet.	2RW				No data			No data
Teleostei								
Trisopterus sculptus (Koken, 1891)	2RW							
Merlangius pseudaeglefinus (Newton, 1891)	1		x	x	x	x	x	No data
Gadiculus benedeni (Leriche, 1926)	3		x	x	x	x		
Gadiculus verticalis (Gaemers & Schwarzhans, 1973)	2		x	x	x	x	x	

(generally <20, Moerdijk et al., 2010, fig. 252), here distinguished as Type 1 (Plate 3.5a–b). Another specimen with ca. 23 relatively flattened ribs is referred to as *Scalaricardita scalaris* - Type 2 (Plate 3.6a–b). While Marquet (2005) and many authors (including Glibert, 1957) distinguished a third species (*Cyclocardia orbicularis orbicularis*), Janssen & Moerdijk (2004) considered the latter synonymous with *S. chamaeformis.* Following the criteria outlined by these authors, specimens IST 6670, IST 6672 and possibly IST 6673 of Marquet (2005, plate 13, fig. 1a, c, d, e, f) represent *S. scalaris* - Type 1 due to the convexity of their lunula, while specimen IST 6671 (Marquet, 2005, fig. 1b, g) resembles *S. chamaeformis* forma *orbicularis* due to the distant narrow ribs and the markedly prosogyrate umbo. Whether the informal Type 1 and Type 2 of *S. scalaris* are subspecies or formae remains undecided, given the insufficient amount of material from layer O to assess the natural variation.

8. Discussion and conclusions

8.1. Berchem Formation - Kiel Member

The lower part of the Rubenshuis outcrop (layers A-B-C) shows the typical, fairly homogeneous, fine- to medium-fine-grained sandy facies of the Kiel Member as observed elsewhere in the city of Antwerp (Everaert et al., 2020; Louwye et al., 2023a). Higher in the Kiel Member (layers D-E-F), the lithology becomes more atypical due to an interval with increased silt content and the presence of well-preserved *Glycymeris* (Fig. 2). This makes it even somewhat resemble the facies of the overlying Antwerpen Member. The similarity in granulometry between the silty interval of the Kiel Member and the Antwerpen Member is consistent with the similar SBT parameters within SBT sequence 4 (Fig. 7). Despite this similarity, the CPTs still shows the typical qc drop from the Kiel Member towards the Antwerpen Member (Fig. 6), as noticed by Deckers & Everaert (2022) while correlating CPTs and outcrops in eastern Antwerp. North of the city of Antwerp, similar silty intervals have also been noticed sporadically by Deckers et al. (2023a) in the upper part of the Kiel Member in boreholes. On top of the silty interval in the Rubenshuis section, layer G again resembles the more classic facies, allowing the Kiel and Antwerpen members to be distinguished in the field by their typical colour difference, identical to all nearby sections (Hoedemakers & Dufraing, 2018; Everaert et al., 2019, 2020).

The silty interval of the Kiel Member up to the basal part of the Antwerpen Member exhibits soft-sediment deformation attributed to load casting. In temporary outcrops within the city of Antwerp, “simple load casts” are frequently observed at the base of the Antwerpen Member, deforming the top of the Kiel Member in case of extreme collapses (Everaert et al., 2020). Furthermore, we present some examples of what could be other, minor deformation structures such as attached and detached pseudonodules. Deckers et al. (2023a) quantified the lithological difference between both members in temporary outcrops, revealing that the lower part of the Antwerpen Member contains significantly more silt (16% silt) compared to the dominant facies of the Kiel Member (3% silt). This contrast in lithology may have generated the reversed density gradient necessary for the formation of load casts at the boundary between both members. It also explains why pronounced load casting is present in the silty upper interval of the Kiel Member at the Rubenshuis outcrop. Additionally, a typical example of load casting was drawn in the upper part of the Antwerpen Member near Borgerhout (Janssen, 1987; Supplementary data: Fig. S2), again occurring at the interface between weakly silty, “medium fine to medium coarse” sand on top of “medium coarse” sand. Also further north at the Verrebroekdok section, Goolaerts (2000) and Deckers et al. (2020) noted load casting of the more clayey/silty Lillo Formation into the top of the Kattendijk Formation. Nevertheless, the occurrence of lithological contrasts alone is not enough to elucidate these deformation structures, necessitating a specific trigger to induce liquefaction. In general, such triggers include seismicity, irregular loading, and cyclic pore pressure fluctuations caused by storm waves (Molina et al., 1998; Owen, 2003). The regional unconformity and hiatus encompassing parts of the DN3 zone between the Kiel and Antwerpen members in the city of Antwerp led Everaert et al. (2020) to associate the load casts at this level with a local palaeogeographical rearrangement phase. However, this hypothesis remains speculative and warrants further investigation, particularly in relation to other load casts in the Neogene of the Antwerp area.

The dinocyst analyses of the Kiel Member in the Rubenshuis outcrop are consistent with previous analyses in Louwye et al. (2000, 2020a) and Everaert et al. (2020). As concluded in the latter study, all samples containing macrofossils are part of biozone DN2 (early–middle Burdigalian). Similarly to the Post X section in Berchem, the upper half metre of the Kiel Member in the Rubenshuis section belongs to late Burdigalian DN3 zone. In contrast, the maximum thickness of the DN3 zone is 6 metres in the southern “Grote Steenweg” (AG) outcrop (Louwye et al., 2000). Therefore, although a laterally increasing hiatus develops within the top of the Kiel Member (Everaert et al., 2020, fig. 11), thin remnants of the upper Burdigalian are still present in the city centre.

The boundary between the DN2 and DN3 zones in the Rubenshuis outcrop is lithologically very different from the boundary in the Argenta and Post X outcrops (informally described as *Cordiopsis* horizon). The biostratinomy of all fossil concentrations in the Kiel Member indicates a shallow depositional environment (probably less than 25 m) above the storm wave base, where currents, storm flows and (storm) waves influenced the shoreface (Everaert et al., 2020; this study). In such shallow facies, lateral variation is not surprising. The formation of shell beds and fossil concentrations is a complex interplay of multiple factors, several formative processes can overprint each other’s signature, blurring single events. The biofabric thus mainly records the final concentration process (Fürsich & Oschmann, 1993). For example, according to Everaert et al. (2020), the shells in the “*Glycymeris-Cyrtodaria* horizon” (Argenta outcrop) were exposed to a high-energy environment with low sedimentation rates for a prolonged period, while the final biofabric was generated by reworking and transport through storm-induced currents during “a single storm phase”. While the signature of the latter seems dominant in the final biofabric, it is clear that such shell beds are actually shaped by a multitude of successive storm phases and/or currents over a larger possible time scale, ranging from a few weeks to possibly thousands of years (see Kidwell & Bosence, 1991, fig. 9).

Some collected macrofossils refine our knowledge of the palaeontology of the Berchem Formation. For example, *Ennucula haesendoncki haesendoncki* is found for the first time in the Kiel Member. Hence, this subspecies has been occurring in the Miocene of Antwerp for at least 1.8 Ma longer than previously known. Besides, tumid specimens of *Glossus lunulatus* cf. *lunulatus* are also encountered. These are morphologically similar to specimens known from the Lower Miocene of Rumst/Terhagen (Gaemers *in* Vinken, 1988; Herman & Marquet, 2007; pers. obs. SE). Given the middle Burdigalian age derived from dinocysts in these deposits, these specimens form an intermediate stage in the lineage from

Glossus lunulatus crassus in the early Burdigalian Edegem Member to the typical *Glossus lunulatus lunulatus* in the Langhian Antwerpen Member.

8.2. Berchem Formation - Antwerpen Member

The interval of the Antwerpen Member has a similar lithology as elsewhere in Antwerp. A typical horizon is the so-called "basal shell bed", layer I in the Rubenshuis outcrop. It is continuous over the different outcrops (Fig. 9). Slightly higher in the Antwerpen Member, phosphatic concretions are usually present. This is indeed the case in layers K and M, half a metre above layer I. Hence, layers K and M are probably correlative with the so-called "*Ptychidia eryna* phosphatic horizon", as described in earlier studies (see Louwye et al., 2010; Hoedemakers & Dufraing, 2018; Everaert et al., 2020; S2 in Deckers & Everaert, 2022; Hoedemakers & Marquet, 2024) (Fig. 9). In these studies, the species was assigned to the genera *Turritella* and *Haustator*. However, the biostratinomy in the Rubenshuis outcrop differs from other outcrops (e.g. Argenta and Tweelingenstraat sections), as layers K and M contain more fine shells instead of stacked *Glycymeris* and much less phosphorite. The phosphatic zone has been interpreted as the (first) maximum flooding surface of the Antwerpen Member (Everaert et al., 2020; Deckers & Everaert, 2022), which is consistent with a calm depositional history of gradual biogenic accumulation with less influence from currents and storms inferred for layers K and M.

The dinoflagellate cyst association of the basal Antwerpen Member in the Rubenshuis outcrop (sample Ru-I) indicates the presence of the late Burdigalian DN3 biozone, a zone previously not recognised in all other outcrops of the Antwerpen Member (see Louwye et al., 2000, 2010, 2020a; Everaert et al. 2020). Due to the lowest occurrence of *Labyrinthodinium truncatum*, the basal Antwerpen Member always holds the early Langhian DN4 biozone (Fig. 9), which is recognised 45 cm higher in the section (sample Ru-K). Further biostratigraphic and lithostratigraphic analysis can elucidate whether the relative

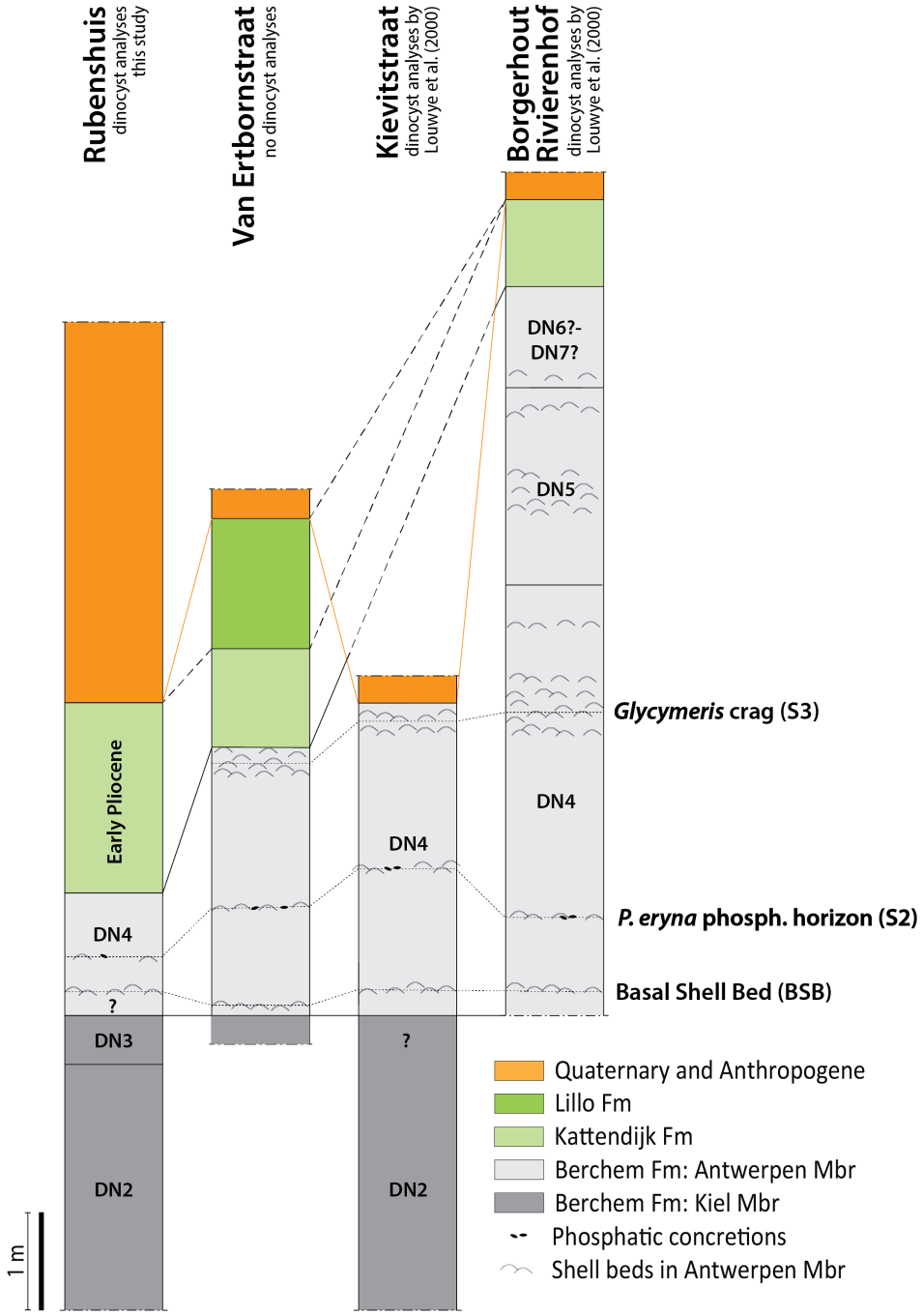

Figure 9. Correlation of the Rubenshuis outcrop with nearby temporary outcrops described by De Meuter et al. (1976) near the Lange Kievitstraat and Borgerhout-Rivierenhof, and Hoedemakers & Marquet (2024) near the Van Ertbornstraat (see Fig. 1). Dinocyst analyses by Louwye et al. (2000) and this study. Characteristic shell beds of the Antwerpen Member are indicated.

dating of sample Ru-I as late Burdigalian is caused by reworking through burrowing from the subjacent Kiel Member sediments.

8.3. Kattendijk Formation

The basal gravel of the Kattendijk Formation contains abundant, well-preserved fossils reworked from the Antwerpen Member, which is indicative of erosion of the former into the latter. Indeed, the thickness of the Antwerpen Member is strongly reduced (1.1 m). Even the most erosion-resistant interval of the Antwerpen Member has been removed, the so-called "*Glycymeris* crag" in its central part (S3 in Deckers & Everaert, 2022; Deckers & Goolaerts, 2022). A few hundred metres to the east of the Rubenshuis, at the Van Ertbornstraat outcrop (Fig. 1), this "*Glycymeris* crag" was still described just below the Kattendijk Formation by Hoedemakers & Marquet (2024) (Fig. 9). The Van Ertbornstraat section is very similar to the Rubenshuis outcrop. Reworked shells from the Antwerpen Member were also mentioned from the base of the (slightly thinner) Kattendijk Formation (Hoedemakers & Marquet, 2024). Further towards the northeast at the Borgerhout – Rivierenhof outcrop (Fig. 1), the Kattendijk Formation overlies a 7 m thick succession of the Antwerpen Member, being the most complete section of this member (De Meuter et al., 1976; Deckers & Everaert, 2022) (Fig. 9). These temporary outcrops therefore corroborate the truncation of the Antwerpen Member by the Kattendijk Formation in western direction, as shown by a CPT correlation panel north of the city of Antwerp (Deckers & Louwye, 2020). The entire Berchem Formation was removed northwest of the city of Antwerp where the Kattendijk Formation has a maximum thickness of up to 15 m. Within the thickest succession of the Kattendijk Formation, Deckers and Louwye (2020) noticed a geotechnical two-fold subdivision. Its lower unit represents the infill of a deep gully incision northwest of Antwerp in the Waasland area, while the upper unit was subsequently deposited in a wider, more shallow gully system. The latter, younger gully system also reached the city of Antwerp. This model is supported by the macropalaeontological content of the basal gravel of the Kattendijk Formation in the Rubenshuis outcrop, as the recorded fauna with abundant *Ditrupa* and *Pygocardia rustica tumida* forma *solida* resembles the highest part of the Kattendijk Formation from the Oosterweel outcrop and nearby sections (Ringelé, 1974; Janssen et al., 1984) (Fig. 1). Furthermore, the abundant occurrence of *Laevastarte ariejansseni* was only known before from the younger Luchtbal Member of the Lillo Formation. Considering that the presence and distribution of benthic molluscs is mostly environmentally controlled, it can be argued that the faunal overlap with the Oosterweel section at least indicates a similar facies. On the other hand, the poor faunal overlap with the basal Kattendijk Formation at Kallo/Doel clearly points to different environmental conditions. Therefore, these palaeontological observations reinforce the regional depositional model of the Kattendijk Formation established by Deckers & Louwye (2020), suggesting that only its youngest gully sequence was deposited in the city of Antwerp.

Acknowledgments

We would like to thank several people who contributed to this study. Dimitri De Clerck and Kris Huyghe (both BAM Interbuild) provided access to the Rubenshuis outcrop. We thank the Bureau for Environment and Spatial Development – Flanders, VPO, for financial support. Roel De Koninck (VITO, Mol) assisted in the field. Frank Wesselingh (NBC, Leiden), Ronald Pouwer (NBC, Leiden), Peter Moerdijk (Middelburg) and Aad Bastemeijer (The Hague) helped with the identification of Pliocene molluscs. Frank and Ronald also helped with photographing shells. Kristiaan Hoedemakers (RBINS, Brussels) identified teleost otoliths, and drew our attention to the profile of the Van Ertbornstraat outcrop (June 1996). We thank Rik Houthuys (Halle) for the discussion on the sedimentology. Alfred Uchman (Jagiellonian University, Poland) provided information about ichnofossils. Ray Perreault (Jarreau Scientific, USA) and Alberto Collareta (Università di Pisa, Italy) re-identified the barnacles. Pieter De Schutter (RBINS, Brussels) photographed sediment samples. Katleen Van Baelen (VITO, Mol) did the excellent graphic work for the figures. Annelise Folie (RBINS, Brussels) stored the collected fossils in the RBINS collection. Stijn Goolaerts (RBINS, Brussels) shared his insights on the Kattendijk Formation. Finally, we want to thank the reviewers: Noël Vandenberghe (KU Leuven) and Frank Wesselingh (NBC, Leiden). Their constructive suggestions improved our paper significantly.

Author contributions

SE, JD and MB documented and sampled the temporary outcrop. MB was able to recover and preserve most fossils. MS performed the CPTs at the site, which were further interpreted in collaboration with JD. JD studied and interpreted the soft-sediment deformations. SL performed the palynological analyses and interpretations. Macropalaeontology and biostratinomy were studied by SE. All authors contributed to the writing of this manuscript.

Data availability

All studied fossils are housed in the collection of the Royal Belgian Institute of Natural Sciences (RBINS) guaranteeing their long-term safekeeping and availability to other researchers for future studies. The palynological slides are stored at Ghent University (Department of Geology). Sediment (sub)samples are stored at the Geological Survey of Belgium (BGD) and the Geotheek of the Flemish Department of the Environment (VPO).

References

Bosch, J. & Wesselingh, F., 2006. On the stratigraphic position of the Delden Member (Breda Formation, Overijssel, the Netherlands) with implications for the taxonomy of Pygocardia (Mollusca, Bivalvia). Cainozoic Research, 4/1-2, 109–117.

Cogels, P., 1874. Observations géologiques et paléontologiques sur les différents dépôts rencontrés à Anvers lors du creusement des nouveaux bassins. Annales de la Société malacologique de Belgique, 9, 7–32.

Deckers, J. & Everaert, S., 2022. Distinguishing the Miocene Kiel and Antwerpen Members (Berchem Formation) and their characteristic horizons using Cone Penetration Tests in Antwerp (northern Belgium). Geological Journal, 57, 2129–2143. https://doi.org/10.1002/gj.4384

Deckers, J. & Everaert, S., 2023. Boring 1434-B-G227574-9_Kapellen3_WVP27. Lithologische beschrijving. Databank Ondergrond Vlaanderen. https://www.dov.vlaanderen.be/data/interpretatie/2023-368900, accessed 28/01/2024.

Deckers, J. & Goolaerts, S., 2022. Cone Penetaration Test characterization of middle and upper Miocene lithostratigraphic units near Antwerp International Airport. Geologica Belgica, 25/3-4, 89–98. https://doi.org/10.20341/gb.2022.002

Deckers, J. & Louwye, S., 2020. The architecture of the Kattendijk Formation and the implications on the early Pliocene depositional evolution of the southern margin of the North Sea Basin. Geologica Belgica, 23/3-4, 323–331. https://doi.org/10.20341/gb.2020.017

Deckers, J., Louwye, S. & Goolaerts, S., 2020. The internal division of the Pliocene Lillo Formation: correlations between Cone Penetration Tests and lithostratigraphic type sections. Geologica Belgica, 23/3-4, 333–343. https://doi.org/10.20341/gb.2020.027

Deckers, J., De Koninck, R., Everaert, S., Adriaens, R. & Verhaegen, J., 2023a. Granulometry, carbonate and glauconite content as stratigraphic tools to distinguish the Kiel Member and lower Antwerpen Member (Berchem Formation) in the City of Antwerp area (Belgium). Geologica Belgica, 26, 127–141. https://doi.org/10.20341/gb.2023.008

Deckers, J., Louwye, S., Goolaerts, S. & Everaert, S., 2023b. The Kattendijk Formation, 01/09/2023. National Commission for Stratigraphy Belgium. https://ncs.naturalsciences.be/lithostratigraphy/kattendijk-formation/, accessed 15/03/2024.

de Heinzelin de Braucourt, J., 1950. Stratigraphie pliocène et quaternaire observée au Kruisschans. I. Analyse stratigraphique & II. Conclusions. Institut royal des Sciences naturelles de Belgique, 26/40-41, 1–38 & 1–22.

de Heinzelin de Braucourt, J., 1955. Deuxième série d'observations stratigraphiques au Kruisschans. Coupes de l'écluse Baudoin. I. Analyse stratigraphique & II. Conclusions. Institut royal des Sciences naturelles de Belgique, 31/66-67, 1–29 & 1–14.

De Meuter, F.J. & Laga, P.G., 1976. Lithostratigraphy and biostratigraphy based on benthonic foraminifera of the Neogene deposits of Northern Belgium. Bulletin de la Société belge de Géologie, 85/4, 133–152.

De Meuter, F., Wouters, K. & Ringelé, D., 1976. Lithostratigraphy of Miocene sediments from temporary outcrops in the Antwerp city area: Pl. Antwerpen 28 W, Pl. Borgerhout 28 E. Service géologique de Belgique, Professional Paper, 1976/3, 19 p.

De Schepper, S. & Head M., 2008. Age calibration of dinoflagellate cyst and acritarch events in the Pliocene–Pleistocene of the eastern North Atlantic (DSDP Hole 610A). Stratigraphy, 5/2, 137–161.

De Schepper, S., Head, M. & Louwye, S., 2009. Pliocene dinoflagellate cyst stratigraphy, palaeoecology and sequence stratigraphy of the Tunnel-Canal Dock, Belgium. Geological Magazine, 146/1, 92–112. https://doi.org/10.1017/S0016756808005438

De Schutter, P.J. & Everaert, S., 2020. A megamouth shark (Lamniformes: Megachasmidae) in the Burdigalian of Belgium. Geologica Belgica, 23/3-4, 157–165. https://doi.org/10.20341/gb.2020.001

de Verteuil, L. & Norris, G. 1996. Miocene dinoflagellate stratigraphy and systematics of Maryland and Virginia. Micropaleontology, 42, Supplement, 1–172. https://doi.org/10.2307/1485926

de Verteuil, L. & Norris, G., 1997. Palynological delineation and regional correlation of the lower through upper Mioccene sequences in the Cape May and Atlantic city boreholes, New Jersey Coastal Plain. Proceedings of the Ocean Drilling Program, Scientific Results, 150X, 129–145. http://dx.doi.org/10.2973/odp.proc.sr.150X.310.1997

Dybkjær, K. & Piasecki, S., 2010. Neogene dinocyst zonation for the eastern North Sea Basin, Denmark. Review of Palaeobotany and Palynology, 161/1-2, 1–29. https://doi.org/10.1016/j.revpalbo.2010.02.005

Everaert, S., De Schutter, P., Mariën, G., Cleemput, G., Van Boeckel, J., Rondelez, D. & Bor, T., 2019. Een vroeg-miocene fauna uit het Zand van Kiel (Formatie van Berchem) bij Post X in Berchem (Antwerpen). Afzettingen WTKG, 40, 83–100. https://natuurtijdschriften.nl/pub/1010449

Everaert, S., Munsterman, D., De Schutter, P., Bor, T., Bosselaers, M., Van Boeckel, J., Cleemput, G. & Bor, T.J. 2020. Stratigraphy and palaeontology of the lower Miocene Kiel Sand Member (Berchem Formation) in temporary exposures in Antwerp (northern Belgium). Geologica Belgica, 23/3-4, 167–198. https://doi.org/10.20341/gb.2020.025

Fürsich, F.T. & Oschmann, W., 1993. Shell beds as tools in basin analysis: the Jurassic of Kachchh, western India. Journal of the Geological Society, 150, 169–185. https://doi.org/10.1144/gsjgs.150.1.0169

Glibert, M., 1945. Faune malacologique du Miocène de la Belgique : I. Pélécypodes. Mémoires du Musée royal d'Histoire naturelle de Belgique, 103, 1–266.

Glibert, M., 1957. Pélécypodes du Diestien, du Scaldisien et du Merxemien de la Belgique, deuxième note. Bulletin de l'Institut royal des Sciences naturelles de Belgique 33/47, 1–28.

Goolaerts, S., 2000. Sedimentologische, stratigrafische en paleoecologische studie van de Pliocene en Quartaire afzettingen aangetroffen in fase 2 van het Verrebroekdok, provincie Oost-Vlaanderen. Proefschrift Licentiaat Geologie (unpublished Master Thesis), KULeuven, Leuven, 133 p.

Goolaerts, S., De Ceuster, J., Mollen, F., Gijsen, B., Bosselaers, M., Lambert, O., Uchman, A., Adriaens, R., Van Herck, M., Houthuys, R., Louwye, S., Bruneel, Y., Elsen, J. & Hoedemaekers, K., 2020. The upper Miocene Deurne Member of the Diest Formation revisited: unexpected results from the study of a large temporary outcrop near Antwerp International Airport, Belgium. Geologica Belgica, 23/3-4, 219–252. https://doi.org/10.20341/gb.2020.011

Grémare, A., Sardá, R., Medernach, L., Jordana, E., Pinedo, S., Amouroux, J.M., Martin, D., Nozais, C. & Charles, F. 1998. On the dramatic increase of *Ditrupa arietina* O.F. Müller (Annelida: Polychaeta) along both the French and the Spanish Catalan coasts. Estuarine, Coastal and Shelf Science, 47, 447–457. https://doi.org/10.1006/ecss.1998.0379

Hartley, J.P., 2014. A review of the occurrence and ecology of dense populations of *Ditrupa arietina* (Polychaeta: Serpulidae). Memoirs of Museum Victoria, 71, 85–95. http://doi.org/10.24199/j.mmv.2014.71.09

Harzhauser, M. & Landau, B., 2019. Turritellidae (Gastropoda) of the Miocene Paratethys Sea with considerations about turritellid genera. Zootaxa, 4681/1, 1–136. https://doi.org/10.11646/zootaxa.4681.1.1

Herman, J. & Marquet, R., 2007. Le Miocène du Deurganckdok à Doel. Memoirs of the Geological Survey of Belgium, 54, 1–149.

Herman, J., Crochard, M. & Girardot, M., 1974. Quelques restes de sélaciens récoltés dans les Sables du Kattendijk à Kallo. Bulletin de la Société belge de Géologie, 83, 15–31.

Hoedemakers, K., 2013. Teleost fish otoliths from the Neogene of Mill-Langenboom (province of Noord-Brabant, The Netherlands). Cainozoic Research, 10/1-2, 35–52.

Hoedemakers, K. & Dufraing, L., 2018. Een profiel bij Posthofbrug (Antwerpen). Afzettingen WTKG, 39, 65–80. https://natuurtijdschriften.nl/pub/707391

Hoedemakers, K. & Marquet, R., 2024. Een profiel in pliocene en miocene zanden in de Van Ertbornstraat te Antwerpen. Afzettingen WTKG, 45, 83–89.

Janse, A.C. & Janssen, A.W., 1983. The Mollusc fauna of the Stemerdink bed (Miocene, Reinbekian) from outcrops in the Slinge brook at Winterswijk-Brinkheurne (the Netherlands, province of Gelderland). Mededelingen van de Werkgroep voor Tertiaire en Kwartaire Geologie, 20, 105–140.

Janssen, A.W., 1984. Mollusken uit het Mioceen van Winterswijk-Miste: een inventaris, met beschrijving en afbeelding van alle aangetroffen soorten. Koninklijke Nederlandse Natuurhistorische Vereniging, Nederlandse Geologische Vereniging, Rijksmuseum van Geologie en Mineralogie, Leiden, 451 p.

Janssen, A.W., 1987. Borgerhout, Kleine Ring, E-3 (23-9-1987), n.v. afslag Borgerhout. Unpublished drawings. Cenozoic Mollusc Collection, Naturalis Biodiversity Center, Leiden.

Janssen, A.W. & Moerdijk, P.W., 2004. Revision of Pliocene representatives of Cyclocardia (Bivalvia, Carditidae) from the North Sea Basin. Basteria, 68, 77–85.

Janssen, A.W. & Van der Mark, D., 1968. Einleitung zu den Beiträgen zur Kenntnis der Molluskenfauna des jüngeren Tertiärs im Nordseebecken. Basteria, 32, 76–82.

Janssen, A.W., Peeters, G.A. & Van der Slik, L., 1984. De fossiele schelpen van de Nederlandse stranden en zeegaten, * (slot). Basteria, 48, 89–200.

Janssen, R., 2014. A review of the Oligocene Limopsidae of the North Sea Basin (Mollusca: Bivalvia). Geologica Saxonica, 61, 1, 7–33.

Kidwell, S.M., 1989. Stratigraphic condensation of marine transgressive records: Origin of major shell deposits in the Miocene of Maryland. The Journal of Geology, 97/1, 1–24. https://doi.org/10.1086/629278

Kidwell, S.M. & Bosence, D.W.J., 1991. Taphonomy and time-averaging of marine shelly faunas. In Allison, P.A. & Briggs, D.E.G. (eds), Taphonomy: Releasing the Data Locked in the Fossil Record. Plenum Press, New York, 115–209.

Kidwell, S.M., Fürsich, F.T. & Aigner, T., 1986. Conceptual framework for the analysis and classification of fossil concentrations. Palaios, 1, 228–238. https://doi.org/10.2307/3514687

Kondo, Y., Abbott, S.T., Kitamura, A., Kamp, P J., Naish, T.R., Kamataki, T. & Saul, G.S., 1998. The relationship between shellbed type and sequence architecture: examples from Japan and New Zealand. Sedimentary Geology, 122/1-4, 109–127. https://doi.org/10.1016/S0037-0738(98)00101-8

Laga, P., 1972. Stratigrafie van de mariene Plio-Pleistocene afzettingen uit de omgeving van Antwerpen met een bijzondere studie van de foraminiferen. Unpublished Ph.D. Thesis. Katholieke Universiteit Leuven - Faculteit Wetenschappen, Leuven, 3 vol., 252 p.

Louwye, S., 2005. The Early and Middle Miocene transgression at the southern border of the North Sea Basin (northern Belgium). Geological Journal, 40, 441–456. https://doi.org/10.1002/gj.1021

Louwye, S. & Deckers, J., 2023. The Berchem Formation, 01/09/2023. National Commission for Stratigraphy Belgium. http://ncs.naturalsciences.be/lithostratigraphy/Berchem-Formation, accessed 15/03/2024.

Louwye, S., De Coninck, J. & Verniers, J., 2000. Shallow marine Lower and Middle Miocene deposits at the southern margin of the North Sea Basin (northern Belgium): dinoflagellate cyst biostratigraphy and depositional history. Geological Magazine, 137, 381–393. https://doi.org/10.1017/s0016756800004258

Louwye, S., Head, M. & De Schepper, S., 2004. Dinoflagellate cyst stratigraphy and palaeoecology of the Pliocene in northern Belgium, southern North Sea Basin. Geological Magazine, 141/3, 353–378. https://doi.org/10.1017/S0016756804009136

Louwye, S., Marquet, R., Bosselaers, M. & Lambert, O. 2010. Stratigraphy of an Early–Middle Miocene Sequence near Antwerp in Northern Belgium (Southern North Sea Basin). Geologica Belgica, 13, 269–284.

Louwye, S., Deckers, J., Verhaegen, J., Adriaens, J. & Vandenberghe, N., 2020a. A review of the lower and middle Miocene of northern Belgium. Geologica Belgica, 23/3-4, 137–156. https://doi.org/10.20341/gb.2020.010

Louwye, S., Deckers, J. & Vandenberghe, N., 2020b. The Pliocene Lillo, Poederlee, Merksplas, Mol and Kieseloolite Formations in northern Belgium: a synthesis. Geologica Belgica, 23/3-4, 297–313. https://doi.org/10.20341/gb.2020.016

Louwye, S., Adriaens, R., Deckers, J., Everaert, S., Vandenberghe, N. & Verhaegen, J., 2023a. The Kiel Member, 01/09/2023. National Commission for Stratigraphy Belgium. http://ncs.naturalsciences.be/lithostratigraphy/Kiel-Member, accessed 15/03/2024.

Louwye, S., Adriaens, R., Deckers, J., Everaert, S., Vandenberghe, N. & Verhaegen, J., 2023b. The Antwerpen Member, 01/09/2023. National Commission for Stratigraphy Belgium. http://ncs.naturalsciences.be/lithostratigraphy/Antwerpen-Member, accessed 15/03/2024.

Marquet, R., 1984. A remarkable Molluscan fauna from the Kattendijk Formation (Lower Pliocene) at Kallo (Oost-Vlaanderen, Belgium). Bulletin de la Société belge de Géologie, 93, 335–345.

Marquet, R., 1991. Recent temporary exposures of the Antwerpen Sands in the Antwerp City area: stratigraphy and fauna. Contributions to Tertiary and Quaternary Geology, 28, 9–12.

Marquet, R., 1998. De Pliocene gastropodenfauna van Kallo (OostVlaanderen, België). Publicatie van de Belgische Vereniging voor Paleontologie vzw, 17, 246 p.

Marquet, R., 2002. The Neogene Amphineura and Bivalvia (Protobranchia and Pteriomorphia) from Kallo and Doel (Oost–Vlaanderen, Belgium). Palaeontos, 2, 1–100.

Marquet, R., 2004. Ecology and evolution of Pliocene bivalves from the Antwerp Basin. Bulletin de l'Institut royal des Sciences naturelles de Belgique, Sciences de la Terre, 74 supplément, 205–212.

Marquet, R., 2005. The Neogene Bivalvia (Heterodonta and Anomalodesmata) and Scaphopoda from Kallo and Doel (Oost-Vlaanderen, Belgium). Palaeontos, 6, 1–142.

Marquet, R. & Herman, J., 2009. The stratigraphy of the Pliocene in Belgium. Palaeofocus, 2, 1–39.

Moerdijk, P.W., Janssen, A.W., Wesselingh, F.P., Peeters, G.A., Pouwer, R., Van Nieulande, F.A.D., Janse, A.C., Van der Slik, L., Meijer, T., Rijken, R., Cadée, G.C., Hoeksema, D., Doeksen, G., Bastemeijer, A., Strack, H., Vervoenen, M. & Ter Poorten, J.J., 2010. De fossiele schelpen van de Nederlandse kust. Nederlands Centrum voor Biodiversiteit Naturalis, Leiden, 294 p.

Molina, J.M., Alfaro, P., Moretti, M. & Soria J.M., 1998. Soft-sediment deformation structures induce by cyclic stress of storm waves in tempestites (Miocene, Guadalquivir Basin, Spain). Terra Nova, 10, 145–150. https://doi.org/10.1046/j.1365-3121.1998.00183.x

Moorkens, T., 1969. Excursions in some temporary outcrops 1966-1969 of the Neogene succession of Antwerp. University of Ghent, Ghent, 45 p.

Munsterman, D. & Deckers, J., 2020. The Oligocene/Miocene boundary in the ON-Mol-1 and Weelde boreholes along the southern margin of the North Sea Basin, Belgium. Geologica Belgica, 23/3-4, 127–135. https://doi.org/10.20341/gb.2020.007

Munsterman, D.K., Van den Bosch, M., Wesselingh, F.P., Helwerda, M. & Busschers, F.S., 2024. A proposal for an updated and revised stratigraphical framework of the Miocene in the Achterhoek (eastern Netherlands). Netherlands Journal of Geosciences, 103, e7. https://doi.org/10.1017/njg.2024.3

Norris, R.D., 1986. Taphonomic gradients in shelf fossil assemblages: Pliocene Purisima Formation, California. Palaios, 1/3, 256–270. https://doi.org/10.2307/3514689

Owen, G., 2003. Load structures: gravity-driven sediment mobilization in the shallow subsurface. Geological Society, London, Special publications, 216, 21–34. https://doi.org/10.1144/GSL.SP.2003.216.01.03

Pérez, D.E. & Giachetti, L.M., 2020. Is *Cyclocardia* (Conrad) a wastebasket taxon? Exploring the phylogeny of the most diverse genus of the Carditidae (Archiheterodonta, Bivalvia). Palaeontology, 63, 477–495. https://doi.org/10.1111/pala.12467

Pouwer, R. & Rijken, R., 2022. De fossiele schelpen van de Nederlandse kust II, deel 16. Naticidae. Spirula, 430, 30–38.

Ringelé, A., 1974. Bijdrage tot de systematiek, de evolutie en de paleoecologie van Bivalvia uit Neogene afzettingen van Noord-België. Unpublished Ph.D. Thesis, Katholieke Universiteit Leuven, Leuven, 280 p.

Robertson, P.K., 1990. Soil classification using the cone penetration test. Canadian Geotechnical Journal, 27/1, 151–158. https://doi.org/10.1139/t90-014

Robertson, P.K., 2010a. Soil behaviour type from the CPT: an update. 2nd International Symposium on Cone Penetration Testing, Huntington Beach, CA, USA, Vol. 2, 575–583.

Robertson, P.K., 2010b. Estimating in-situ soil permeability from CPT and CPTu. 2nd International Symposium on Cone Penetration Testing, Huntington Beach, CA, USA, Vol. 2, 535–542.

Schiaparelli, S., Albertelli, G. & Cattaneo-Vietti, R., 2006. Phenotypic plasticity of Vermetidae suspension feeding: a potential bias in their use as Biological Sea-Level Indicators. Marine Ecology, 27/1, 44–53. https://doi.org/10.1111/j.1439-0485.2006.00076.x

Schiltz, M., 2020. On the use of CPTs in stratigraphy: recent observations and some illustrative cases. Geologica Belgica, 23/3-4, 399–411. https://doi.org/10.20341/gb.2020.019

Stein, G., Moths, H., Albrecht, F., Havekost, U. & Fehse, D., 2016. Revision der Miozänen Molluskenfauna (Hemmoorium) von Werder bei Achim (Nordwest-Niedersachsen). Palaeofocus, 5, 289 p.

Van den Broeck, E., 1892. Matériaux pour la connaissance des dépôts Pliocènes supérieurs rencontrés dans les derniers travaux de creusement des Bassins Maritimes d'Anvers : Bassin Africa (ou Lefebvre) et Bassin America. Bulletin de la Société belge de Géologie, de Paléontologie et d'Hydrologie, 6, Mémoires, 86–149.

Vervoenen, M., 1995. Taphonomy of some Cenozoic Seabeds from the Flemish Region, Belgium. Belgische Geologische Dienst, Professional paper, 1994/5, 272, 115 p.

Vescogni, A., Bosellini, F.R., Reuter, M. & Brachert, T.C., 2008. Vermetid reefs and their use as palaeobathymetric markers: New insights from the Late Miocene of the Mediterranean (Southern Italy, Crete). Palaeogeography, Palaeoclimatology, Palaeoecology, 267, 89–101. https://doi.org/10.1016/j.palaeo.2008.06.008

Vinken, R. (ed.), 1988. The Northwest European Tertiary Basin. Geologisches Jahrbuch, Reihe A, 100, 508 p.

Williams, G.L., Fensome, R.A. & MacRae, R.A., 2017. The Lentin and Williams index of fossil dinoflagellates 2017 edition. American Association of Stratigraphic Palynologists Contributions Series, 48, 1097 p.

Zullo, V.A. & Perreault, R.T., 1989. Review of *Actinobalanus moroni* (Cirripedia, Archaeobalanidae), with the description of new Miocene species from Florida and Belgium. Tulane Studies in Geology and Paleontology, 22, 1–12.

Supplementary data for this paper are available online at https://doi.org/10.20341/gb.2024.005.

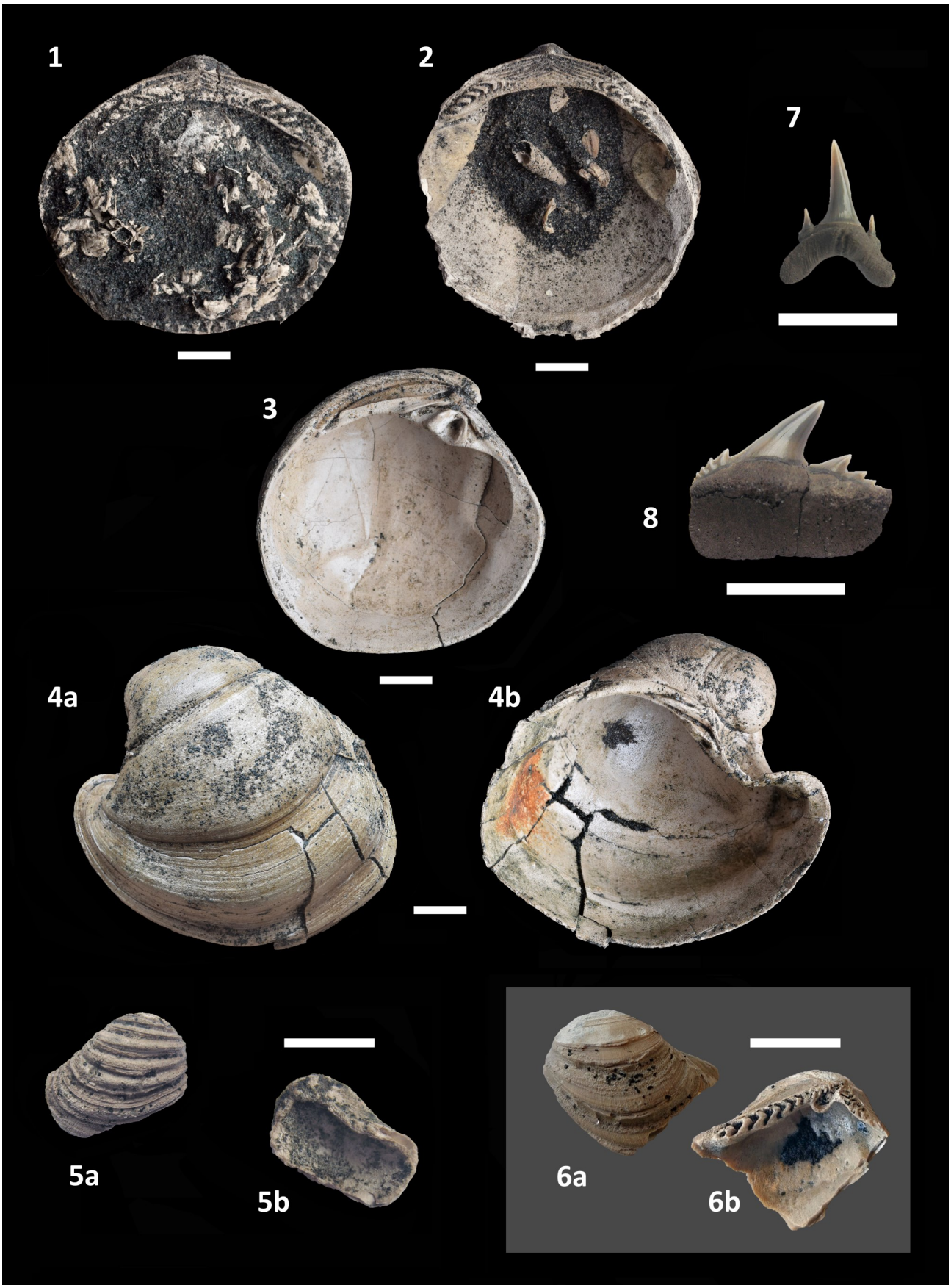

Plate 1. Palaeontology of the Kiel Member (Berchem Formation) (Miocene, middle Burdigalian). **1.** *Glycymeris obovata baldii* Glibert & Van de Poel, 1965 with both articulated and disarticulated *Actinobalanus collinsi* Zullo & Perreault, 1989. RBINS 7737. **2.** *G. baldii* with *A. collinsi*, a specimen of *Ptychidia eryna* (d'Orbigny, 1852) and an otolith of *Trisopterus sculptus* (Koken, 1891). RBINS 7738. **3.** *Cordiopsis polytropa nysti* (d'Orbigny, 1852). RBINS 7739. **4a-b.** *Glossus lunulatus* cf. *lunulatus* (Nyst, 1835). RBINS 7740. **5a-b.** *Ennucula haesendoncki haesendoncki* (Nyst & Westendorp, 1839). RBINS IG 7741. **6a-b.** *Ennucula haesendoncki haesendoncki* (Nyst & Westendorp, 1839). Geotheek (VPO). **7.** *Carcharias gustrowensis* (Winkler, 1875). RBINS P 10760. **8.** *Notorynchus primigenius* (Agassiz, 1835). RBINS P 10761. Specimens 1–5 are from layer E, while specimens 7–8 are from layer B (Rubenshuis outcrop). Specimen 6 was found in the Kiel Member at a depth of 80 m in a PIPDA borehole in Kapellen (DOV 1434-B-G227574-9_Kapellen3_WVP27). Scale bar 10 mm.

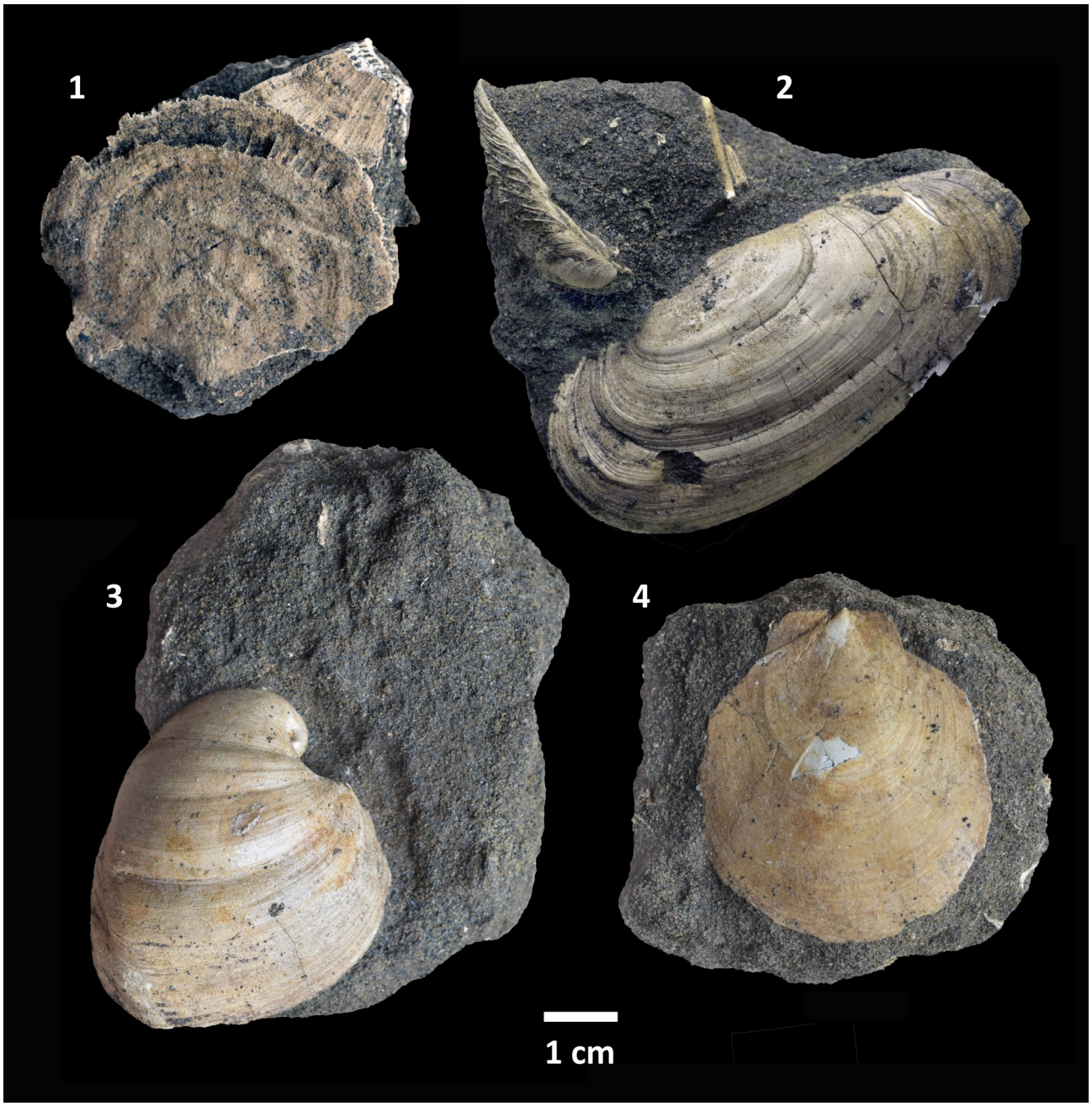

Plate 2. Palaeontology of the Antwerpen Member (Berchem Formation) (Miocene, early Langhian). **1.** *Flabellum tuberculatum* Keferstein, 1857. RBINS 7742. **2.** Articulated *Panopea kazakovae* Glibert & Van de Poel, 1966 in life position, *Venus multilamella multilamella* (Lamarck, 1818) and two echinoid spines. RBINS 7743. **3.** *Glossus lunulatus lunulatus* (Nyst, 1835), classic morphology for the Antwerpen Member. RBINS 7744. **4.** *Korobkovia woodi* (Nyst, 1861). RBINS 7745. All specimens are found within layers K-L-M (Rubenshuis section). Scale bar 10 mm.

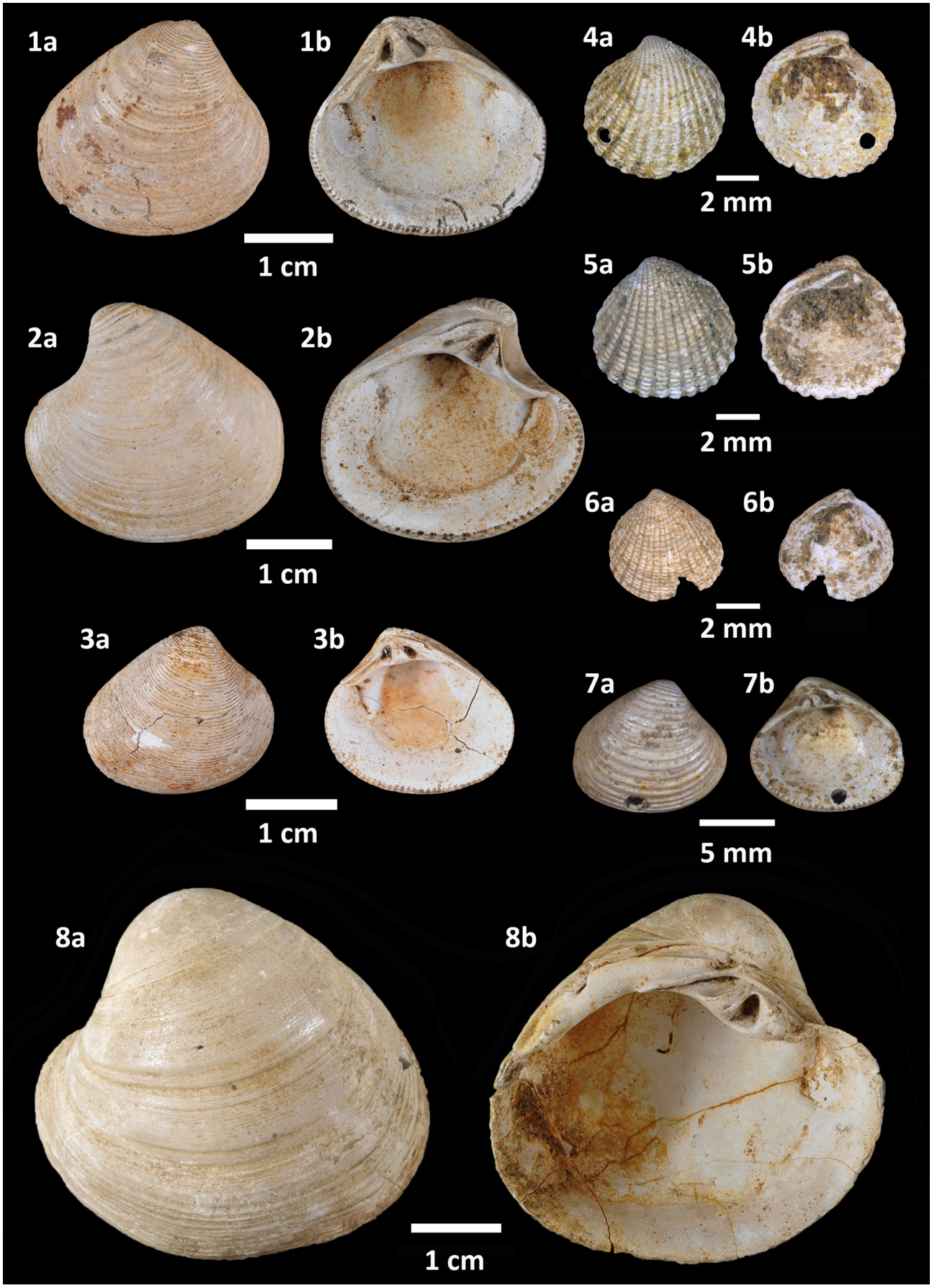

Plate 3. Palaeontology of the Kattendijk Formation (Pliocene, Zanclean). **1.** *Laevastarte ariejansseni* (Marquet, 2005). RBINS 7746. **2.** *Laevastarte omalii omalii* (De la Jonkaire, 1823). RBINS 7747. **3.** *Digitariopsis obliquata burtinea* (De la Jonkaire, 1823). RBINS 7748. **4.** *Scalaricardita chamaeformis* (Sowerby, 1825) forma *orbicularis*. RBINS 7749. **5.** *Scalaricardita scalaris* (Sowerby, 1825) – Type 1. RBINS 7750. **6.** *Scalaricardita scalaris* (Sowerby, 1825) – Type 2. RBINS 7751. **7.** *Astarte corbuloides* De la Jonkaire, 1823. RBINS 7752. **8.** *Pygocardia rustica tumida* (Nyst, 1836) forma *solida*. RBINS 7753. All specimens are found in the basal gravel of the Kattendijk Formation, layer O (Rubenshuis section). The scale bar is indicated for each specimen.